Expected Forward Progress and Throughput of Multi-Hop Frequency-Hopped Spread-Spectrum Networks

by

E. Geraniotis and J.W. Gluck

EXPECTED FORWARD PROGRESS AND THROUGHPUT OF MULTI-HOP FREQUENCY-HOPPED SPREAD-SPECTRUM NETWORKS

Jeffrey W. Gluck and Evaggelos Geraniotis

Department of Electrical Engineering
University of Maryland
College Park, MD 20742

ABSTRACT

Secondary multiple-access interference processes are characterized for multi-hop packet radio networks, in which users are assumed to be Poisson-distributed in the plane and to use frequency-hopped spread-spectrum signaling with a receiver-oriented assignment of frequency-hopping patterns. The throughput per node and the average forward progress are then evaluated for frequency-hopped multi-hop networks which employ (i) random forward routing with fixed transmission radius (RFR) and (ii) most forward progress routing with fixed transmission radius (MFR). The optimal average number of neighbors and transmission radius are derived for these cases when Reed-Solomon forward-error-control coding with minimum distance decoding or binary convolutional coding with Viterbi decoding is employed.

I. INTRODUCTION

In recent years, a good deal of research has been done in the areas of multi-user communication networks and spread-spectrum communications. One of the logical extensions of this research is the use of spread-spectrum techniques in combination with networking techniques in order to provide greater multi-user capabilities and higher resistance to interference, whether hostile or benign. However, there have, thus far, been few attempts to pursue this.

The general feature of most of the spread-spectrum network models proposed to date has been a lack of precision in the characterization of the effects of spread-spectrum techniques on network performance. The general practice in papers like [1] and [2] has been not to pay sufficient attention to the accurate modeling of the effects of spread-spectrum modulation, therefore the results obtained can be very optimistic or pessimistic, depending upon what assumptions are made. In [1], a model is presented for a frequency-hopped (FH) spread-spectrum multiple access (SSMA) digital cellular telephone network, and an expression is derived for throughput. The outstanding features of the model are the characterization of user mobility in terms of a two-dimensional Poisson process and the treatment of transmitter power attenuation with distance. Similar techniques are also used in [2], in which the authors concentrate on trying to model spread-spectrum multi-hop networks and although their multi-hop network model has merit, their treatment of the spread-spectrum modulation is inadequate (they only employ the processing gain without taking into account the characteristics of the specific spread-spectrum modulation).

In contrast, the work of [3] for single-hop frequency-hopped spread-spectrum networks examines in depth the effect of forward-error-control coding and frequency-hopped

spread-spectrum on the throughput and packet error probability of the network which employs a slotted or an unslotted ALOHA protocol. Furthermore, the work of [4] investigates slotted ALOHA protocols with stable throughput for frequency-hopped Reed-Solomon coded single-hop networks. No similar attempts to analyze accurately spread-spectrum multi-hop networks have been made so far.

In this paper, we utilize the spread-spectrum models found in [3], [4], and [8] and incorporate their precise detailed characterizations of the effects of frequency-hopping and forward-error-control coding to the models of multi-hop networks treated in [2], [5] and [6]. The effects of frequency-hopping and forward error-control coding (Reed-Solomon coding with minimum distance decoding or convolutional coding with Viterbi decoding) as well as of data modulation [M-ary (or binary) orthogonal FSK with non-coherent demodulation] are taken into consideration, and the interference processes are characterized accurately in order to evaluate the throughput per node and the average forward progress of the multi-hop network.

An overview of the contents of this paper is as follows. In Section II, results are derived for the throughput per node and the average forward progress for frequency-hopped multi-hop networks with forward-error-control employing random forward routing with fixed transmission radius (RFR), a modification to the scheme treated in [2]. Section III contains results for similar multi-hop networks employing most forward routing with fixed transmission radius (MFR), adapted from [5]. Finally, in Section IV, we present numerical results and conclusions.

II. FREQUENCY-HOPPED MULTI-HOP NETWORKS EMPLOYING RANDOM FORWARD ROUTING WITH FIXED TRANSMISSION RADIUS (RFR)

In this section, expressions are derived for throughput and expected forward progress (which is used to determine optimum transmission ranges) for frequency-hopped multi-hop networks.

The network model to be assumed here is similar to those found in [2], [5] and [6]. A geographically-dispersed network is assumed with a uniform traffic matrix. The number of users in a given area is a two-dimensional Poisson process with density λ users per unit area. Each node is assumed to be able to transmit to users located within some radius R; thus, the average number of "neighbors" (users to whom a given transmitter can transmit) is given by $N = \lambda \pi R^2$. A given node will be in transmit mode with probability p and will not be in transmit mode with probability $1-p$ (this represents a Bernoulli process with parameter p).

The channel access protocol is assumed to be slotted ALOHA, and the system is assumed to utilize frequency-hopping as the means of spreading the spectrum. Receiver-oriented assignment of frequency-hopping patterns is assumed; i.e., a transmitter with a packet to send to some receiver uses the hopping pattern unique to that receiver.

Synchronization at the packet level is assumed feasible for all users. Thus, the uncertainties in the timing between different users are required to be small relative to the packet duration; however, since they might not be small relative to the dwell time of the frequency-hopper, we consider asynchronous frequency-hopping systems. For systems employing Reed-Solomon coding one codeword per packet is transmitted.

There are many possible routing strategies, of which two shall be analyzed here: random forward routing with fixed transmission radius (RFR) analyzed in this section

and most forward routing with fixed transmission radius (MFR) analyzed in the next section.

Random forward routing with fixed transmission radius (RFR) is based on the completely random routing scheme found in [2]. The difference, of course, is that, here, a transmitter always chooses a receiver in the forward direction, the direction in which the ultimate destination is located.

Figure 1 illustrates this strategy and the types of interference that are encountered therein. In the figure, X is transmitting a packet that is destined for node D. X randomly chooses a node Y in the half-circle of radius R surrounding X that is in the direction of node D. Forward progress is denoted by the length of segment $\overline{XZ} = z = r_0\cos\theta_0$.

In the figure, X^1 and X^2 interfere with X's transmission. X^1 is a *primary interferer*; X^1 has a packet destined for D^1, and he randomly chooses Y as his immediate destination node, the same node chosen by X (note that X, likewise, is a primary interferer with X^1's transmission). All primary interferers use the same spread-spectrum code as X uses. X^2 is a *secondary interferer*; X^2 has a packet destined for node D^2 and chooses Y^2 as an intermediate destination. However, since the distance between X^2 and Y is less than R, the fixed transmission radius, some of the signal power used by X^2 is received by Y. The spread-spectrum codes which are used by the secondary interferers are different from the code used by X for transmitting to Y.

In analyzing this scheme, what is desired is the probability that X transmits correctly to some node Y, denoted $P(X\rightarrow Y)$. In order to evaluate this probability, it is necessary to evaluate the probabilities of occurence of a number of contributing events.

Given that a node is in transmit node (with probability p), it actually transmits with probability $1-e^{\frac{N}{2}}$, as discussed in [3], where N is the average number of neighboring nodes (within a circle of radius R), as described above. Thus, we have

$$P_{TX}(X \rightarrow Y) = Pr\,\{X \text{ in transmit mode}\}\cdot Pr\,\{X \text{ can find a receiver } \mid X \text{ in transmit mode}\}$$

$$\cdot Pr\,\{Y \text{ is not in transmit mode}\}$$

$$= p\left(1-e^{-\frac{N}{2}}\right)(1-p). \tag{1}$$

This accounts for the "non-interference" portion of $P(X \rightarrow Y)$; we now concentrate on the interference-related components.

The first piece of information necessary in order to evaluate the interference components is the number of potential interferers (surrounding a receiver). The probability that there are k interfering users (transmitting packets) within a radius R around a given node is given by the Poisson distribution, $P(K=k) = \dfrac{e^{-N}N^{k}}{k\,!}$.

Given that there are k potential interferers, we must now account for the fact that each of these can either not interfere (i.e., not transmit), be a primary interferer, or be a secondary interferer. Let us say that j of these k do interfere; then $k-j$ do not, and this probability is given by $\left[1-p\left(1-e^{-\frac{N}{2}}\right)\right]^{k-j}$. Now, say that i out of the j are primary interferers and $j-i$ are secondary interferers. The probability of this being true can be shown to be $\left(\dfrac{p}{N}\right)^{i}\left[p\left(1-e^{-\frac{N}{2}}\right)-\dfrac{p}{N}\right]^{j-i}$.

The next step involves the evaluation of the probability that X (out of the $i+1$ users transmitting to Y) is captured by the receiver Y and the probability that Y correctly receives the packet of X in the presence of the i primary and $j-i$ secondary

interferers. Regarding capture, we assume that perfect capture occurs; that is, only one

of the contending users will be captured by the receiver, and this event has probability

1. Since $i+1$ users (including X) are contending and each one is equally likely to be

captured by the receiver Y, the probability that Y captures X is $\dfrac{1}{i+1}$. Regarding the

probability of correct reception in the presence of $j-i$ secondary interferers it will be

denoted by $P_c(j-i)$, which, for various coded systems, is given in Appendix A.

Then, summing over all possibilities,

$$P_{I\mid TX}(X\to Y) = \sum_{k=0}^{\infty} \frac{e^{-N}N^k}{k!} \sum_{j=0}^{k} \binom{k}{j} \left[1-p\left(1-e^{-\frac{N}{2}}\right)\right]^{k-j}$$

$$\cdot \sum_{i=0}^{j} \binom{j}{i}\left(\frac{p}{N}\right)^i \frac{1}{i+1}\left[p\,(1-e^{-\frac{N}{2}})-\frac{p}{N}\right]^{j-i} P_c(j-i). \tag{2}$$

We now take our two components, $P_{TX}(X\to Y)$ and $P_{I\mid TX}(X\to Y)$, and get the

overall expression for $P(X\to Y)$. This is simply

$$P(X\to Y) = P_{TX}(X\to Y)P_{I\mid TX}(X\to Y). \tag{3}$$

Unfortunately, the $\dfrac{1}{i+1}$ in $P_{I\mid TX}(X\to Y)$ presents an obstacle in any attempt to

write a closed-form expression for $P(X\to Y)$. However, $\dfrac{1}{i+1}$ can be closely approxi-

mated by a sum of exponentials, $\sum_{\nu} c_\nu e^{\gamma_\nu i}$, in which the c_ν's and γ_ν's can be determined

using Prony's method (see, for example, [7, pp. 378-382]). We have used a three term

approximation in our analysis below and in computing the numerical results shown in

Section IV.

If we further assume that $P_c(j-i)$ can be put in the form $\sum_{m,l} b_{m,l}\, a_{m,l}^{j-i}$ (this is true,

for example, for coded systems, as discussed in Appendix A), then $P(X\to Y)$ can be

expressed in a closed form as

$$P(X \rightarrow Y) = p \left(1-e^{-\frac{N}{2}} \right)(1-p)$$

$$\cdot \sum_{\nu=1}^{3} c_\nu \sum_m \sum_l b_{m,l} \exp\left\{ -pN\left[1-e^{-\frac{N}{2}} - \frac{\delta_\nu}{N} - a_{m,l}\left(1-e^{-\frac{N}{2}} - \frac{1}{N} \right) \right] \right\},$$

$$(4)$$

where $\delta_\nu = e^{\gamma_\nu}$.

In this case, the local normalized throughput (in packets per hop, per node, frequency slot and dimension) is just $\dfrac{r}{q} \dfrac{\log_2 M}{M} P(X \rightarrow Y)$, where we multiplied by $\dfrac{1}{q}$,

$\dfrac{\log_2 M}{M}$ and the forward-error-control (FEC) code rate r that is used to account for the

bandwidth spread. The expected forward progress Z can be shown to be given by

$$Z = \frac{R}{\pi} P(X \rightarrow Y).$$

$$(5)$$

In Appendix A expressions for $P(X \rightarrow Y)$ which permit the evaluation of the

troughput per node and the average forward progress are derived for Reed-Solomon cod-

ing with error-correction decoding and erasure/error-correction minimum distance decod-

ing s well as for binary convolutional codes with side or without side information and

Viterbi decoding.

As an example of a case in which $P_c(j-i)$ is of the form $\sum_{m,l} b_{m,l} a_{m,l}^{j-i}$ which results

in a closed form expression for for $P(X \rightarrow Y)$, we consider the case of RFR with

$RS(n,k)$ coding used along with error-correction decoding. From Appendix A eq. (A.2)

(see also [3]), we notice that we can put $P_c(j-i)$ in the desired form, where

$a_{m,l} = (1-P_h)^{n+l-m}$ and $b_{m,l} = \dbinom{n}{m}\dbinom{m}{l}(-1)^l (1-P_0)^{m_c(n+l-m)}$. Thus, (2) becomes

$$P(X \to Y) = p \left(1 - e^{-\frac{N}{2}} \right) (1-p)$$

$$\cdot \sum_{\nu=1}^{3} c_\nu \sum_{m=0}^{l} \sum_{l=0}^{m} \binom{n}{m} \binom{m}{l} (-1)^l (1-P_0)^{m_c(n+l-m)}$$

$$\cdot \exp \left\{ -pN \left[1 - e^{-\frac{N}{2}} - \frac{\delta_\nu}{N} - (1-P_h)^{n+l-m} \left(1 - e^{-\frac{N}{2}} - \frac{1}{N} \right) \right] \right\}.$$

$$(6)$$

III. FREQUENCY-HOPPED MULTI-HOP NETWORKS EMPLOYING

MOST FORWARD ROUTING WITH FIXED TRANSMISSION RADIUS (MFR)

This strategy differs from RFR in that the node Y that results in the most forward

progress is always chosen by X. This scheme is discussed in [5]. The fact that causes

the analysis of MFR to differ from that of RFR is that, as shown in Figure 2 since Y is

the "most forward" node, there can be no nodes beyond Y in the direction of the desti-

nation; thus, a region, denoted $A(r_0, \theta_0)$ is excluded.

In [5] expressions are derived for $f_{r,\theta}(\cdot,\cdot)$ and $f_z(\cdot)$, the distributions of the position

of the immediate destination node (Y, in the case of X or a primary interferer; some

Y^2, in the case of a secondary interferer). Expressions for the area of $A(r_0, \theta_0)$ are deter-

mined, as well. These are all needed in the evaluation of $P(X \rightarrow Y)$.

As a preliminary to the analysis, define $A'(r_0, \theta_0) = \pi R^2 - A(r_0, \theta_0)$ to be the area

of the non-excluded region. Thus, $N = \lambda \pi R^2$ is the expected number of neighbors in an

entire circle of radius R, while $N'(r_0, \theta_0) = \lambda A'(r_0, \theta_0)$ would be the expected number of

neighbors in the non-excluded region.

The quantities to be determined in this analysis are basically identical to those in

the analysis of RFR, but there are some significant differences. One such difference is

that the Poisson distribution uses $N'(r_0, \theta_0)$, rather than N, in the distribution of the

number of neighbors around Y.

In evaluating the interference probabilities in this case, we will separate the proba-

bility of there being j inteferers out of k potential interferers, given by $\left[p(1 - e^{-\frac{N}{2}}) \right]^j$,

from the probabilities of there being $j-i$ secondary interferers and i primary interferers.

These two quantities are now conditioned on there being j interferers.

If an interferer, say X^1, is a primary interferer, then Y must be X^1's "most forward", node. The overall probability of a node being a primary interferer, given that it is an interferer (i.e., that it transmits and is a neighbor), is given by

$$P_1(R) = Pr\{X^1 \text{ is primary} \mid X^1 \text{ interferes}\}$$

$$= \int_0^R P\{Y \text{ is the most forward neighbor of } X^1 \mid Y \text{ is at radial distance } r_1 \text{ from } X^1\}$$

$$P\{X^1\text{'s radial distance from Y is between } r_1 \text{ and } r_1 + dr_1\} dr_1. \tag{7}$$

Thus, we can write

$$P_1(R) = \int_0^R \frac{2r_1}{R^2} \left[\int_0^{r_1} \int_{-\frac{\pi}{2}}^{\frac{\pi}{2}} f_{r,\theta}(r',\theta') dr' \, d\theta' \right] dr_1, \tag{8}$$

where the term in brackets and $\dfrac{2r_1}{R^2}$, respectively, denote the first and second probability terms in the right member of (7).

The probability that some node, say X^2, is a secondary interferer, given that it is an interferer, is given by the complement of (8); i.e.,

$$Pr\{X^2 \text{ is secondary} \mid X^2 \text{ interferes}\} = P_2(R) = 1 - P_1(R) \tag{9}$$

This quantity represents the sum of the probabilities that Y is not in X^2's forward direction and that Y is in X^2's forward direction but is not "most forward".

As before, we now sum over all possibilities, and, unlike the RFR case, we must now also take the expectation over r_0 and θ_0, the position of the "most forward" node. This gives the following result:

$$P(X \to Y) = p(1 - e^{-\frac{N}{2}})(1-p) \int_0^R \int_{-\frac{\pi}{2}}^{\frac{\pi}{2}} \sum_{k=0}^{\infty} \frac{e^{-N'(r_0,\theta_0)} \left[N'(r_0,\theta_0) \right]^k}{k!}$$

$$\cdot \sum_{j=0}^{k} \binom{k}{j} \left[p\left(1-e^{-\frac{N}{2}}\right) \right]^{j} \left[1-p\left(1-e^{-\frac{N}{2}}\right) \right]^{k-j}$$

$$\cdot \sum_{i=0}^{j} \binom{j}{i} [P_1(R)]^i \frac{1}{i+1} [1-P_1(R)]^{j-i} P_c(j-i)$$

$$\cdot f_{r,\theta}(r_0,\theta_0) d\theta_0 dr_0. \tag{10}$$

In deriving (10), we assumed that capture occurs with probability 1, that is, one of the $i+1$ contending packets is captured by the receiver. Furthermore, if we use the three term exponential approximation to $\frac{1}{i+1}$ and assume that $P_c(j-i)$ is of the form $\sum_{m,l} b_{m,l} a_{m,l}^{j-i}$, as we did in the RFR analysis, the integrand can be simplified to some extent, by evaluating the summations. At the end of this section, we give an example in which this evaluation can be carried out to the end.

Again the normalized local throughput is $\frac{r}{q} \frac{\log_2 M}{M} P(X \rightarrow Y)$ and the expected forward progress can be evaluated by multiplying the integrand in (10) by $r_0 \cos\theta_0$ and then integrating as in (10).

As an example, when Reed-Solomon coding with error-correction minimum distance decoding is employed we can obtain for the MFR case (see Appendix B):

$$P(X \rightarrow Y) = p\left(1-e^{-\frac{N}{2}}\right)(1-p)$$

$$\cdot \sum_{\nu=1}^{3} c_\nu \sum_{m=0}^{t} \sum_{l=0}^{m} \binom{n}{m} \binom{m}{l} (-1)^l (1-P_0)^{m_c(n+l-m)}$$

$$\cdot \int_0^R \int_{-\frac{\pi}{2}}^{\frac{\pi}{2}} \exp\left\{ -pN'(r_0,\theta_0)\left(1-e^{-\frac{N}{2}}\right)\left[1-\delta_\nu P_1(R)-(1-P_h)^{n+l-m}[1-P_1(R)]\right]\right\}$$

$$\int_{r,\theta}(r_0,\theta_0)d\theta_0 dr_0. \tag{11}$$

Expressions similar to (11) can be derived for the case of erasure/error-correction decoding of Reed-Solomon codes, as well as for the Viterbi decoding of binary convolutional codes. These expressions have been derived and cited in Appendices B for the MFR case.

IV. NUMERICAL RESULTS

In this section, results are presented for the normalized throughput per node and the expected forward progress for frequency-hopped multi-hop networks using the RFR and MFR schemes, discussed in Sections II and III, respectively.

The usual performance measures in multi-hop networks (e.g., see [5]-[6]) are: the normalized local throughput defined as $S = \frac{r}{q}\frac{\log_2 M}{M}P(X \to Y)$ (in packets per hop, per node, frequency slot and dimension), the expected forward progress Z (in distance units per hop where Z has the same units as the transmission radius R), and the normalized total throughput γ (in packets per node, frequency slot and dimension), which is defined as $\gamma = Z\ 45\pi\sqrt{\frac{\lambda\pi}{N}}\cdot S$. Notice that the total throughput can be easily obtained from the local throughput and the expected forward progress; we do not present any results on the total throughput in this paper. Also notice that the expected forward progress and the total throughput depend on both λ and N; in contrast, the local throughput depends on λ only through $N = \lambda\pi R^2$, the average number of neighbors.

We start the presentation of results with the RFR case. Figure 3 shows the dependance of Z on N as parametrized by λ. The expected forward progress first increases and then decreases as N increases for fixed λ. As λ increases and N is held fixed, the forward progress decreases because the radius of transmission $R = \sqrt{\frac{N}{\lambda\pi}}$ decreases.

Figures 4(a) and 4(b) show that both S and Z are affected by the value of p; the values increase, then decrease with p. The optimum value of p when N is an unrestricted parameter has been computed to be approximately 0.466 for S in Figure 4(a) and approximately 0.355 for Z in Figure 4(b). The value of $p = 0.1$ appears to provide almost invariant S or Z independent of the value of neighbors N. One thing should be

noted regarding p and λ: these parameters reflect users' behavior and can not, in general, be set to desired values.

Figures 5(a) and 5(b) demonstrate the effects of changing the rate of the code and the decoding algorithm. As shown, throughput decreases significantly when the code rate decreases while it remains invariant for a larger range of N when erasure/error-correction decoding rather than error-correction decoding is employed. In contrast the expected forward progress increases drastically when the code rate decreases and even more so when erasure/error decoding instead of error-only decoding is used. The decrease to throughput due to the decrease in the code rate is due mainly to the normalization of the throughput; that is, the increase in the probability of correct reception due to the lower rate does not balance the penalty of multiplying the throughput by the code rate. On the other hand the expected forward progress does not involve any normalization so that it takes advantage of the full benefit of lower rate coding. In comparing two schemes with similar parameters but error-correction capability (e.g., different code rates or decoding schemes) maintaining a large value of throughput over a broader range is a manifestation of the fact that the one scheme rejects the multiple-access interference better than the other.

Figure 6 shows the behavior of the throughput S as a fuction of N when parametrized by λ for frequency-hopped multi-hop networks employing the binary convolutional code of constrained length 7 and rate 1/2 with no side information available to the decoder. Similar observations as for Figure 3 are in order here. Notice that the values of Z in Figure 6 are smaller than the corresponding values of Figure 3 and for fixed λ they remain invariant with respect to N in a smaller range.

Figures 7(a) and 7(b) show S and Z, respectively, as functions of N when parametrized by p for the same binary convolutional code as above. In particular, Figure 7(a) shows the same trends as Figure 4(a) does; the difference lies in that the convolutional code provides larger peak throughput (for fixed p) but it maintains it for a smaller range of N than the Reed-Solomon code. In contrast, Figure 7(b) shows that the convolutional code both provides a smaller peak expected forward progress and it maintains for a smaller range of N than the Reed-Solomon code.

Figures 8(a) and 8(b) show S and Z, respectively, as functions of N for binary convolutional codes of rates 1/2 and 1/3 and constraint lengths 7 and 9. We observe that decreasing the rate of the code lowers the throughput and increases drastically the average expected progress. Increasing the constraint length improves the performance of the network in terms of both the throughput and the average expected forward progress.

Figures 9(a) and 9(b) provide a comparison of S and Z, respectively, as functions of N for the rate 1/2 binary convolutional codes of constraint lengths 7 and 9 and the Reed-Solomon code (32,16); binary FSK modulation with noncoherent demodulation and hard decisions are employed. Figure 9(a) shows that although the peak throughput of the convolutional-coded network is slightly larger than that of the Reed-Solomon-coded network, the Reed-Solomon-coded network maintains a larger value of the throughput for a broader range of values of N. Then, as Figure 9(b) shows the RS-coded network is far superior to the corresponding convolutional-coded networks in terms of both the peak value and the range of N for which the peak value is approximately maintained of the expected forward progress Z.

We now move on to discuss the results for the MFR case. Figures 10(a) and 10(b) are analogous to Figures 4(a) and 4(b); they show the throughput and expected forward

progress, respectively, parameterized by p. The same trends that appear in the RFR case also appear here in the MFR case.

Figures 11(a) and 11(b) show the throughput and the expected forward progress for two Reed-Solomon-coded networks with code rates 1/2 and 1/4. The throughput of the RS(32,16)-coded network is higher than that of the RS(32,8)-coded system for most values of N this is reversed for N larger than 80. On the other hand the expected forward progress of the lower code-rate scheme is higher than that of the higher code-rate scheme for all values of N.

Finally, Figures 12(a) and 12(b) compare RFR and MFR performance in terms of throughput and average expected progress, respectively, for a given set of parameters. In Figure 12(a), it is shown that the RFR scheme with RS(32,16) and error-only decoding outperforms in terms of peak throughput value the corresponding MFR schemes with the same RS coding and error-only or erasure/error decoding; however the MFR schemes maintain a large value of the throughput for broader range of values of N and between the two the erasure/error decoding scheme is superior. Then in Figure 12(b) it is shown that the MFR scheme outperforms the corresponding RFR scheme and that for MFR schemes the value of Z can improve considerably by using erasure/error decoding.

V. CONCLUSIONS

We have presented here an analysis of a model for randomly-distributed frequency-hopped multi-hop networks. The aspect of this analysis which differs most from previous analyses of multi-hop spread-spectrum networks is the characterization of other-user interference and its mitigation by the use of spread-spectrum techniques (frequency-hopping here). We have also been able to incorporate the effects of modulation, coding, and noise into the analysis.

The numerical results presented show network performance (normalized local throughput and expected forward progress) as a function of the average number of neighbors around a node. Variations in performance are demonstrated for variatins in probability of a user being in transmit mode, density of users in the plane, and coding employed. These results also compare the two types of routing, RFR and MFR, considered in the analysis.

An obvious extension of this work would be to consider deterministic, rather than randomly-distributed, networks. This would not involve a major modification to the analysis; it would involve removing the Poisson-related elements in the analysis and is, thus, rather trivial. However, it would be somewhat more difficult were one to consider non-identical nodes, i.e., nodes with different transmitter powers (or, similarly, to account for signal attenuation with distance).

The importance of this work should not be underemphasized; however, there remains much to be done in the area of spread-spectrum multi-hop networks. The analysis here does not deal with issues like spreading code protocols and access protocol stability. With so many unsolved problems, this remains a fertile area of research.

REFERENCES

[1] Verhulst, D., Mouly, M., and Szpirglas, J., "Slow Frequency Hopping Multiple Access for Digital Cellular Radiotelephone," *IEEE Journal on Selected Areas in Communications*, Vol. SAC-2, No. 4, July, 1984.

[2] Sousa, E., and Silvester, J., "Determination of Optimum Transmission Ranges in a Multihop Spread Spectrum Network," *Proc. MILCOM '85*, Boston, MA, November, 1985.

[3] Pursley, M., "Throughput of Frequency-Hopped Spread-Spectrum Communications for Packet Radio Networks," *Proc. of the 1983 Conf. on Information Sciences and Systems*, The Johns Hopkins University, pp. 550-556, March 1983; also "Frequency-hop transmission for satellite packet switching and terrestrial packet radio networks", *IEEE Trans. on Information Theory*, Vol. IT-32, pp. 652-667, September 1986.

[4] Hajek, B., "Recursive Retransmission Control--Aplication to a Frequency-Hopped Spread-Spectrum System," *Proc. of the 1983 Conf. on Information Sciences and Systems*, The Johns Hopkins University, pp. 116-120, March 1982.

[5] Hou, T.-C., and Li, V., "Transmission Range Control in Multihop Packet Radio Networks," *IEEE Trans. on Communications*, Vol. COM-34, No. 1, January 1986.

[6] L. Kleinrock and J. A. Silvester, "Optimum transmission radii for packet radio networks or why six is a magic number," in Confer. Record of *National Telecommunications Conference*, pp. 4.3.1 - 4.3.5, December 1978.

[7] Hildebrand, F. B., *Introduction to Numerical Analysis*, New York: McGraw Hill, 1956.

[8] Geraniotis, E. A., and Pursley, M. B., "Error Probabilities for Slow-Frequency-Hopped Spread-Spectrum Multiple-Access Communications Over Fading Channels," Special Issue on Spread-Spectrum Communications of the *IEEE Trans. on Communications*, Vol. COM-30, pp. 996-1009, May 1982.

[9] Berlekamp E. R., "The technology of error-correcting codes," *Proc. IEEE*, Vol. 68, pp. 564-593, May 1980.

[10] J. Conan, "The weight spectra of some short low-rate convolution~'
Trans. on Communications, Vol. COM-32, pp. 1050-1053, S~~·
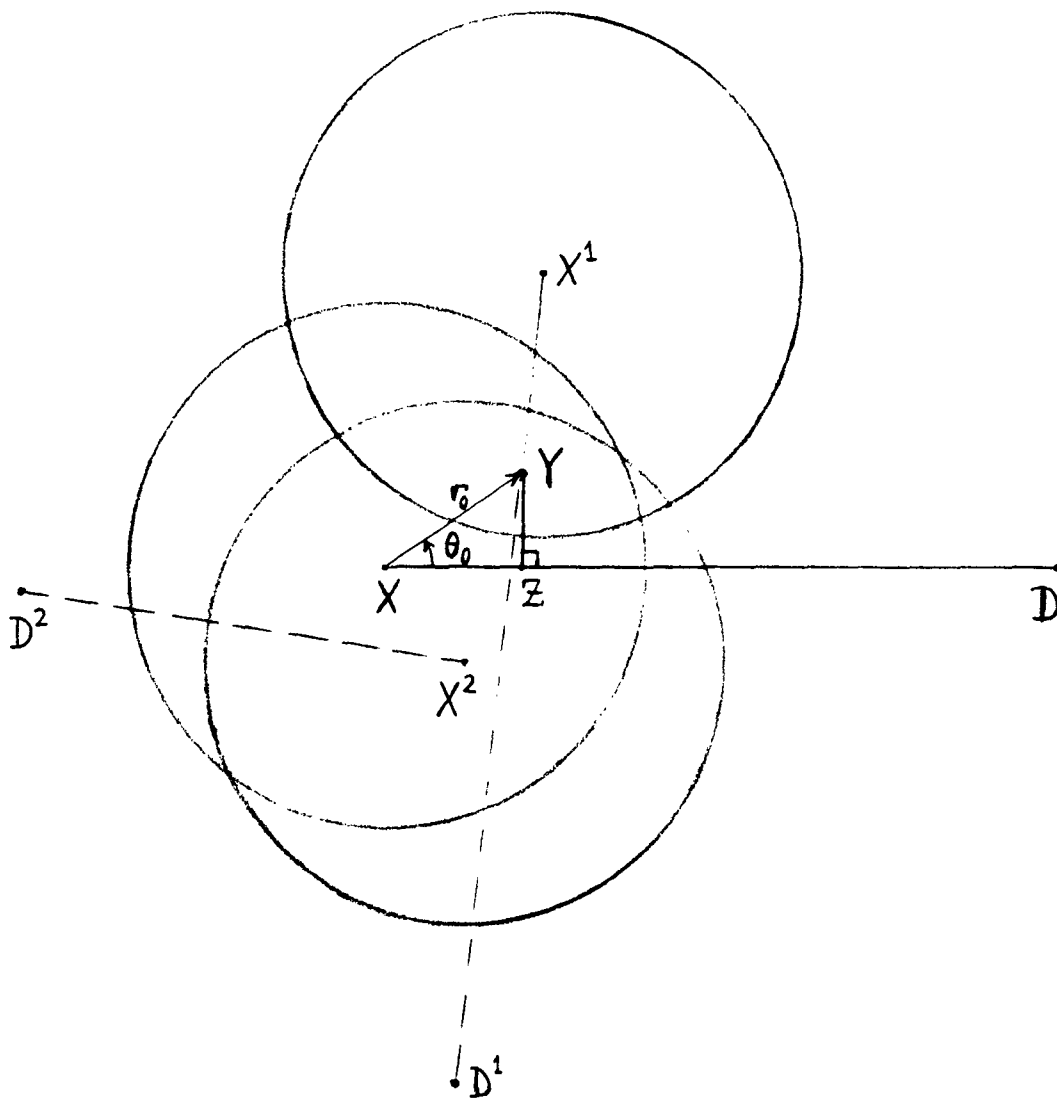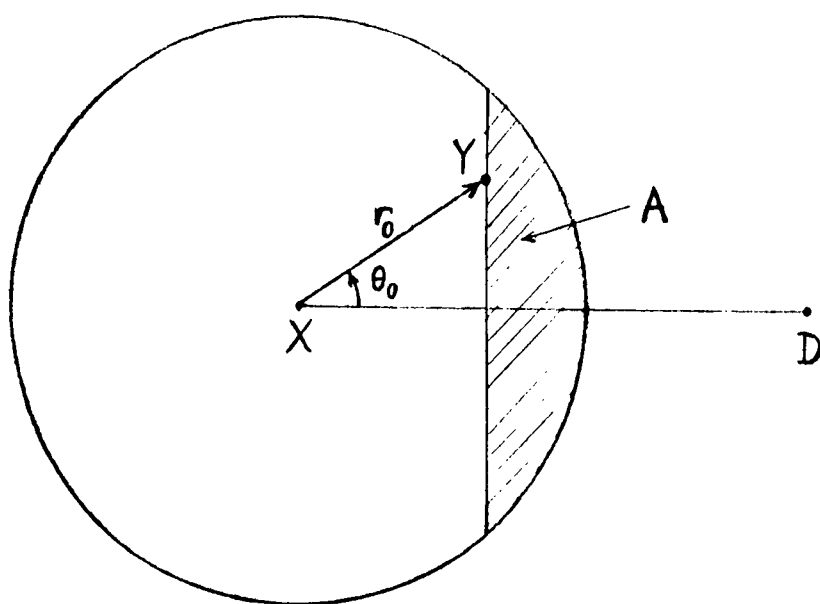
Figure 1. Interference in Random Forward Routing

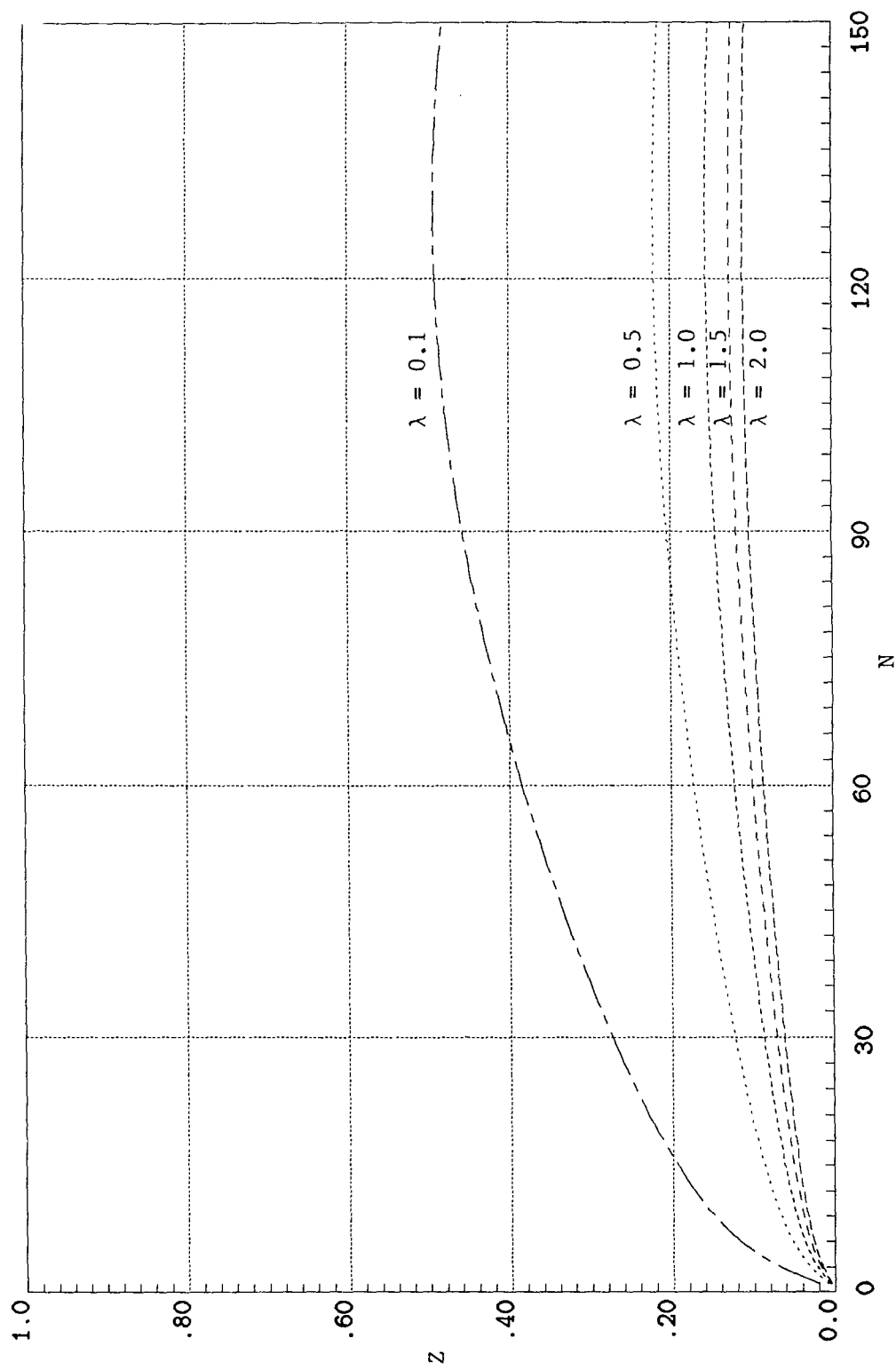Figure 2. Excluded Region in Most Forward Routing with Fixed
Transmission Radius

Figure 3. Expected Forward Progress versus Average Number of Neighbors for Various λ (RFR, p=0.1, RS(32,16) coding with error-only decoding, q=100, N_b=10, SNR=20 dB, AWGN, 32-ary FSK with non-coherent demodulation, asynchronous).

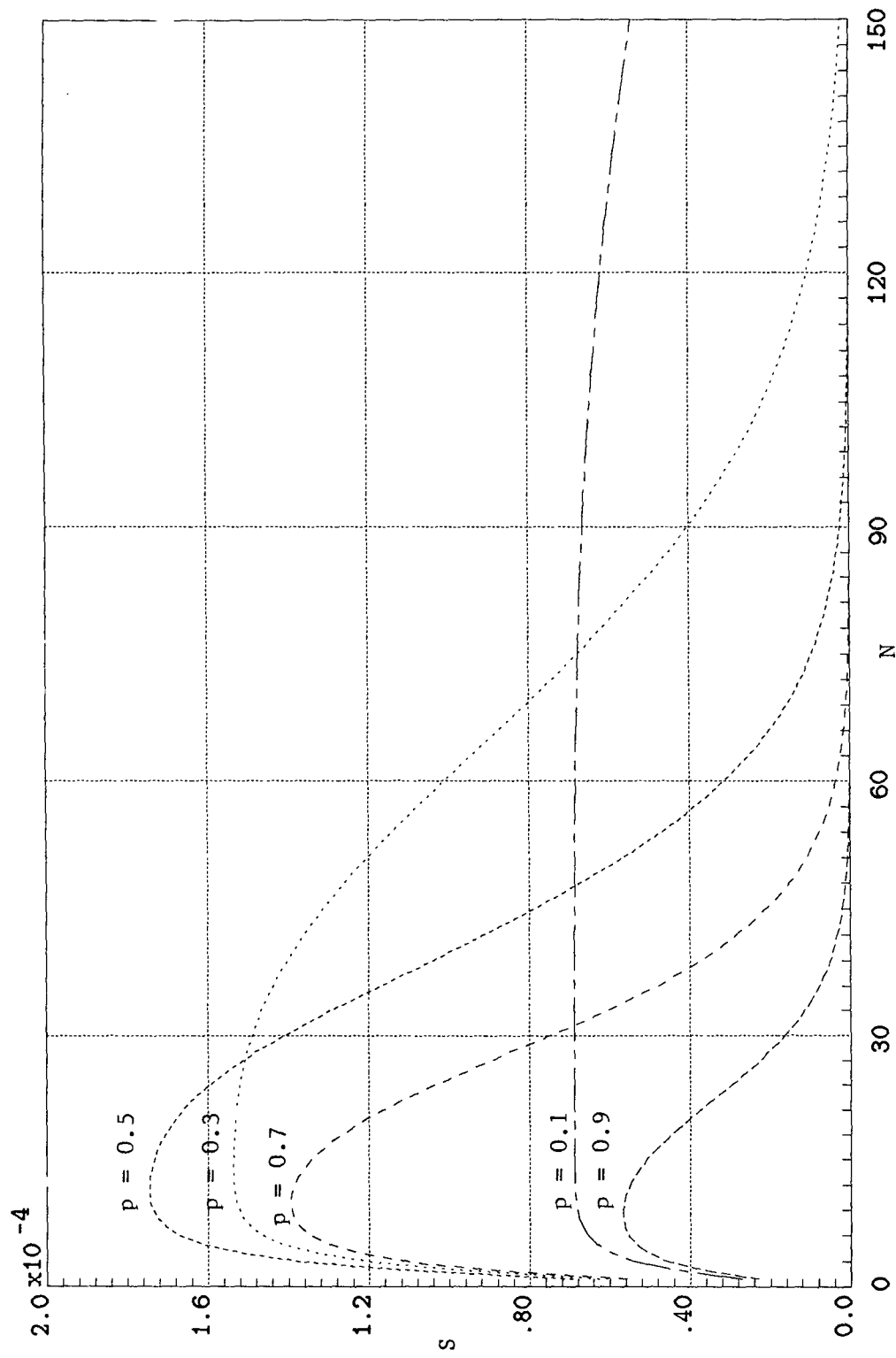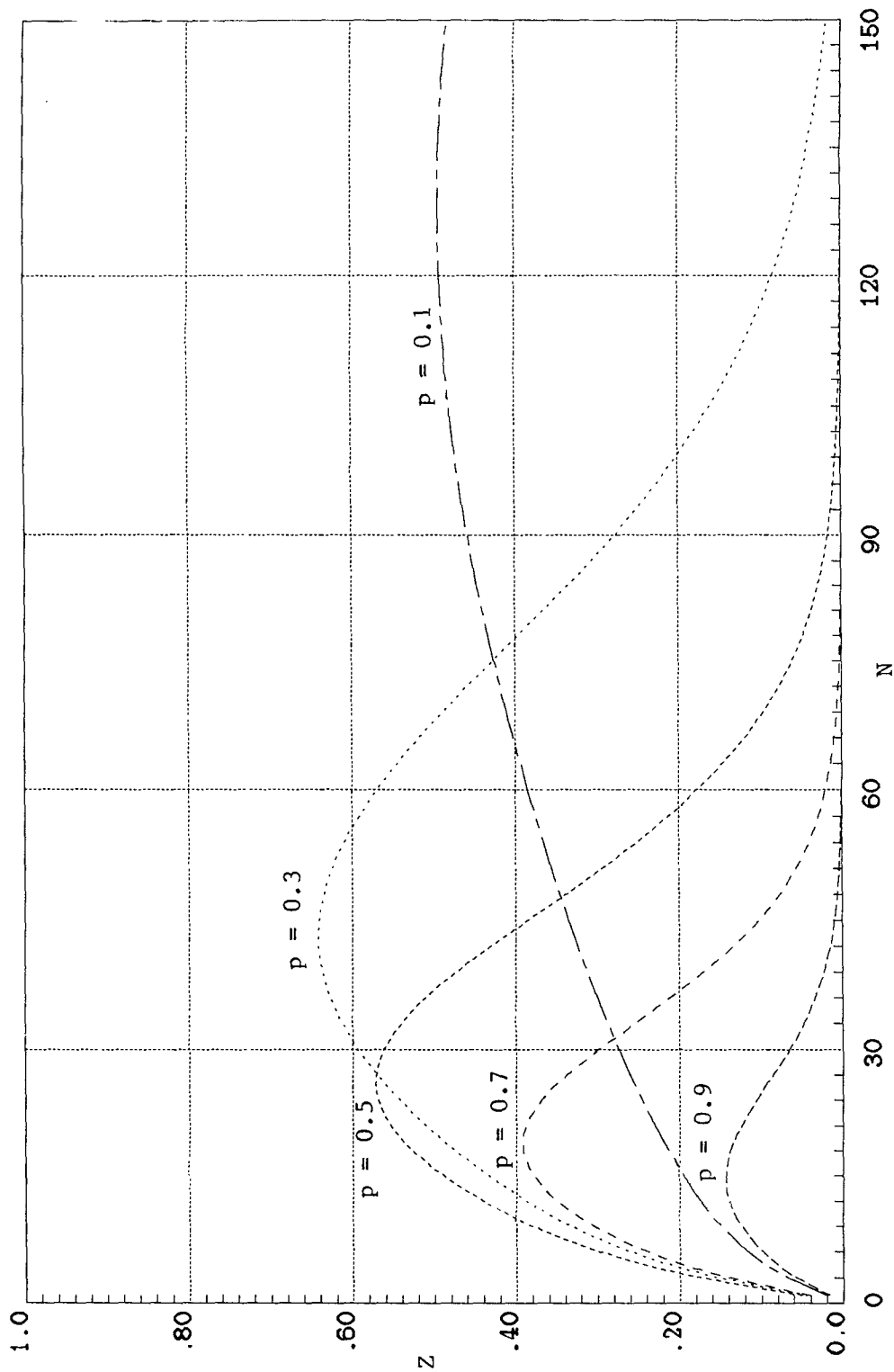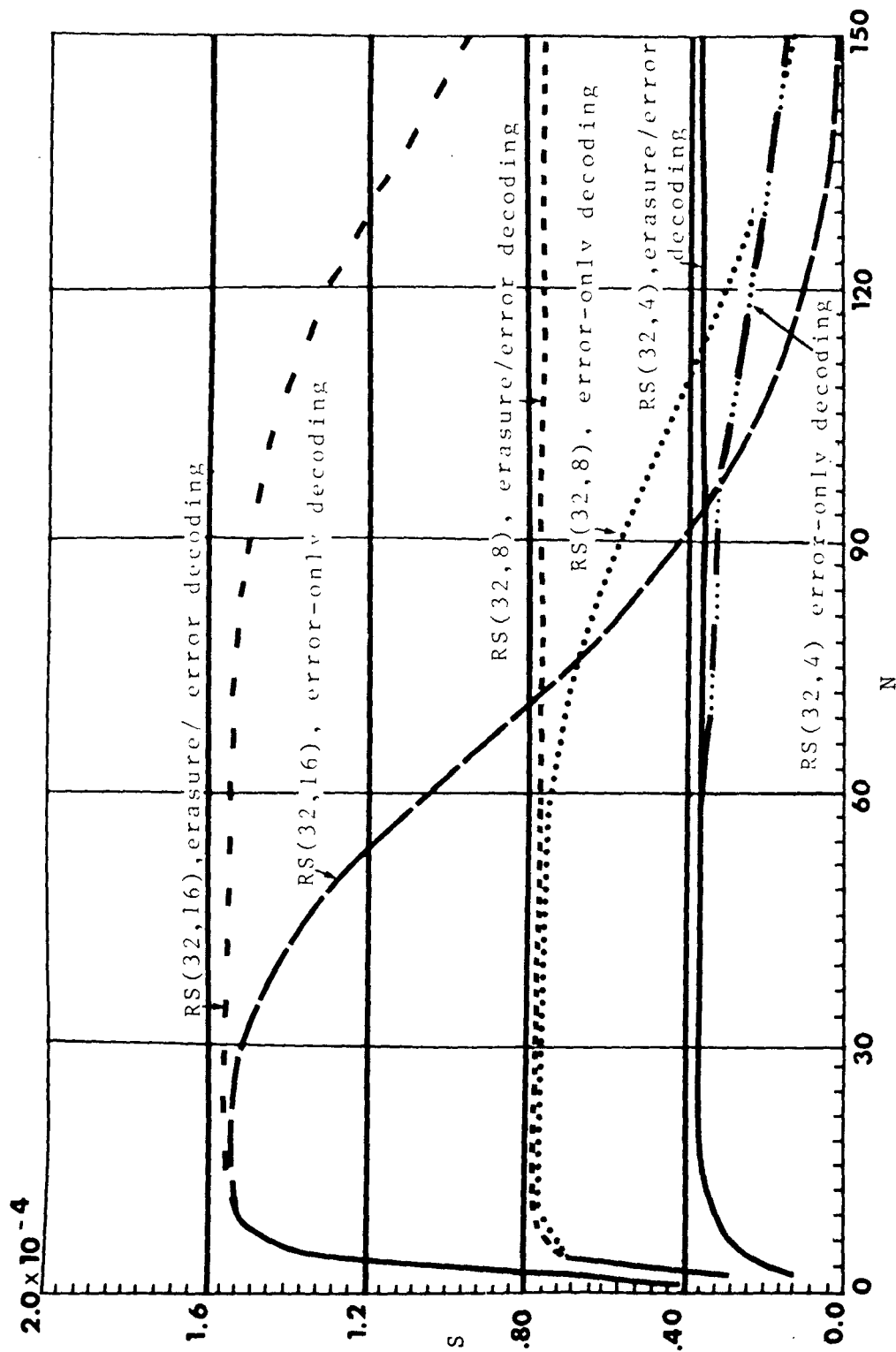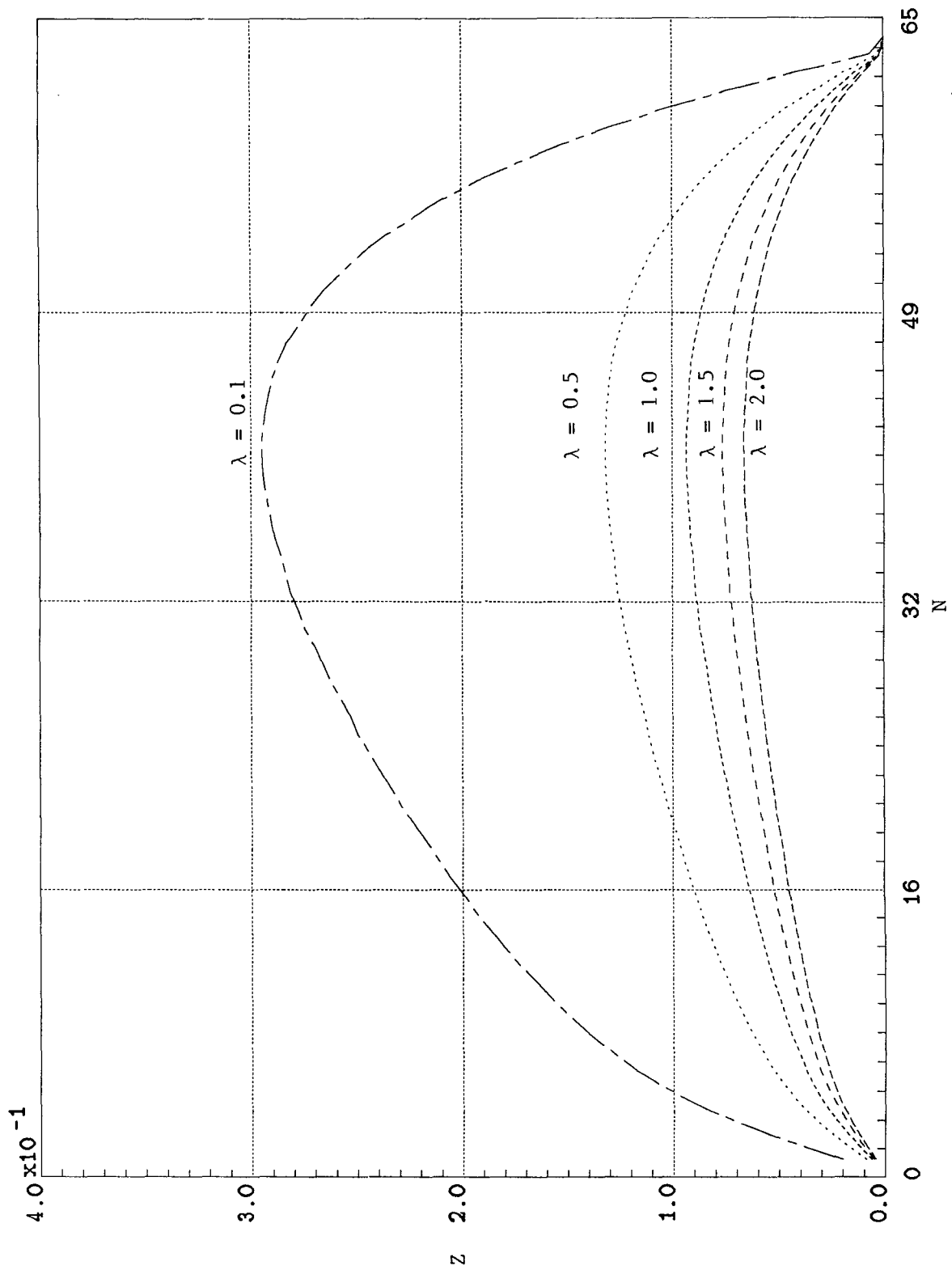Figure 4(a). Throughput versus Average Number of Neighbors for Various p (RFR, $\lambda=0.1$, RS(32,16) coding with error-only correction decoding, q=100, $N_b=10$, SNR=20 dB, AWGN, 32-ary FSK with non-coherent demodulation, asynchronous).

Figure 4(b). Expected Forward Progress versus Average Number of Neighbors for Various p (RFR, $\lambda=0.1$, RS(32,16) coding with error -only correction decoding, q=100, $N_b=10$, SNR=20 dB, AWGN, 32-ary FSK with non-coherent demodulation, asynchronous).

Figure 5(a). Throughput versus Average Number of Neighbors for Various Reed-Solomon Code Rates and Decoding Schemes (RFR, $p=0.3$, $\lambda=0.1$, $q=100$, $N_b=10$, SNR=20 dB, AWGN, 32-ary FSK with non-coherent demodulation, asynchronous).
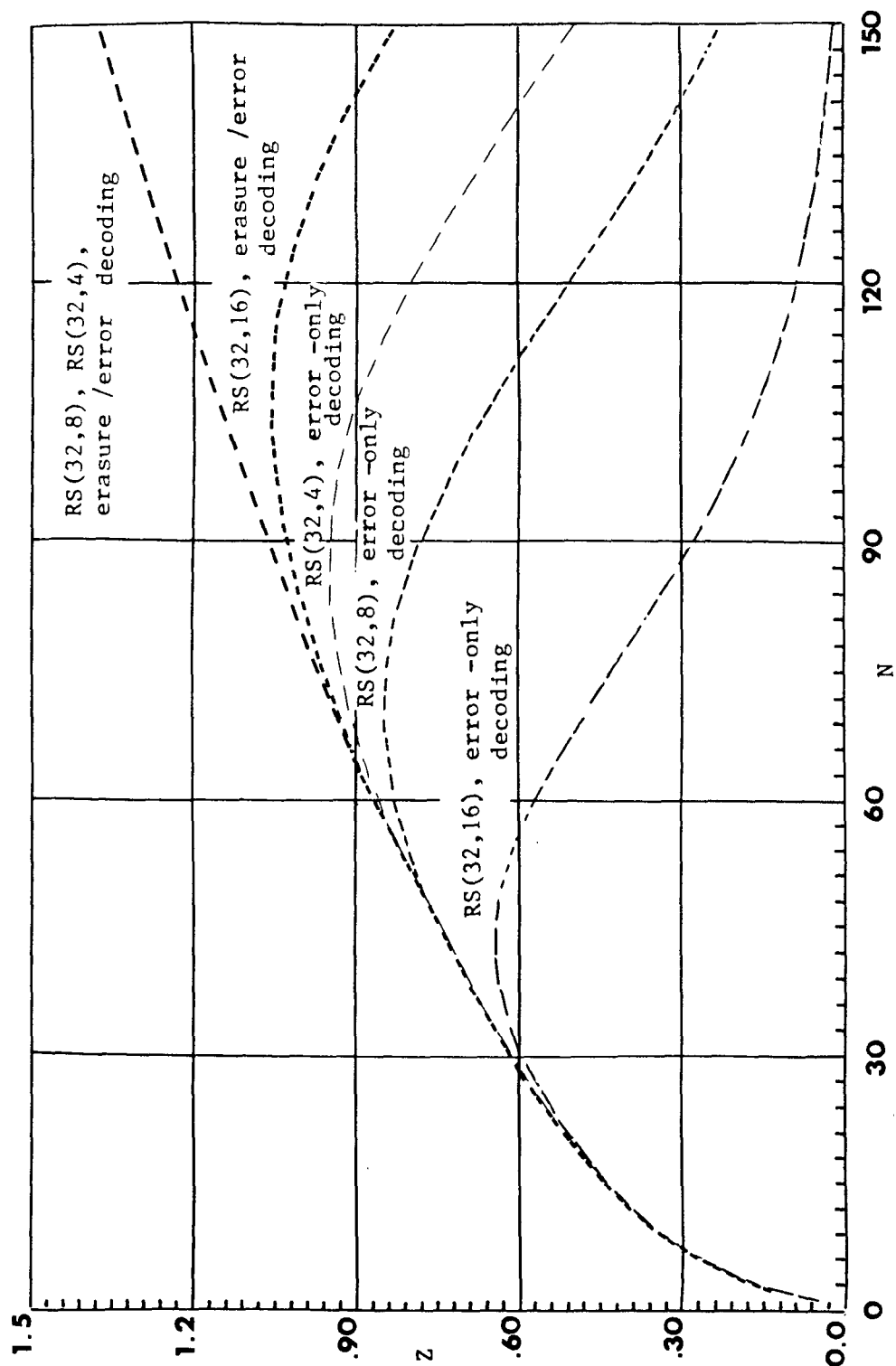
Figure 5(b). Expected Forward Progress versus Average Number of Neighbors for Various Reed-Solomon Code Rates and Decoding Schemes (RFR, p=0.3, λ=0.1, q=100, N_b=10, SNR=20 dB, AWGN, 32-ary FSK with non-coherent demodulation, asynchronous).
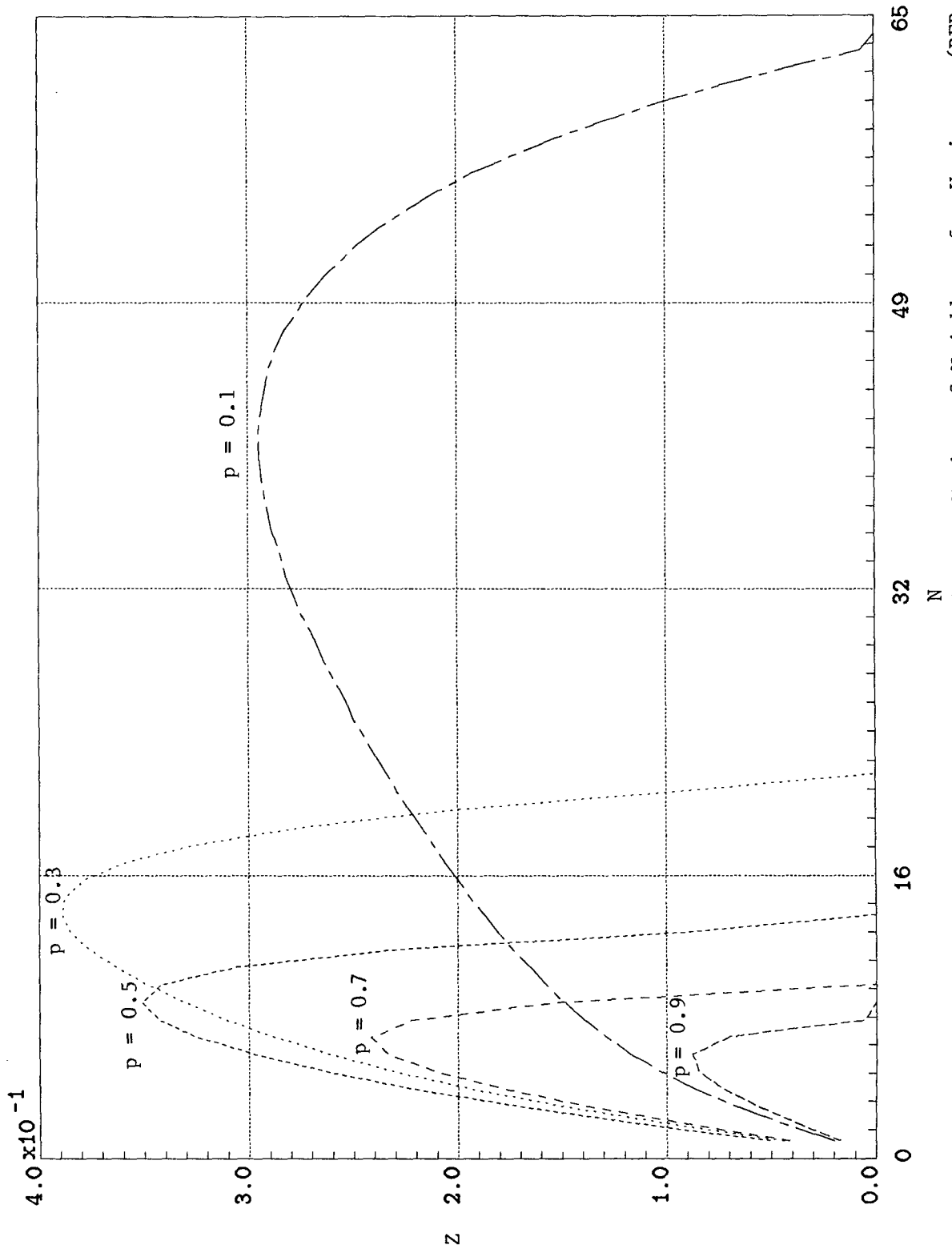
Figure 6.   Expected Forward Progress versus Average Number of Neighbors for Various λ (RFR, p=0.1, CC(7,1/2) coding with no side information available to the decoder, q=100, N_b=10, SNR=20 dB, AWGN, binary FSK with non-coherent demodulation, asychronous).
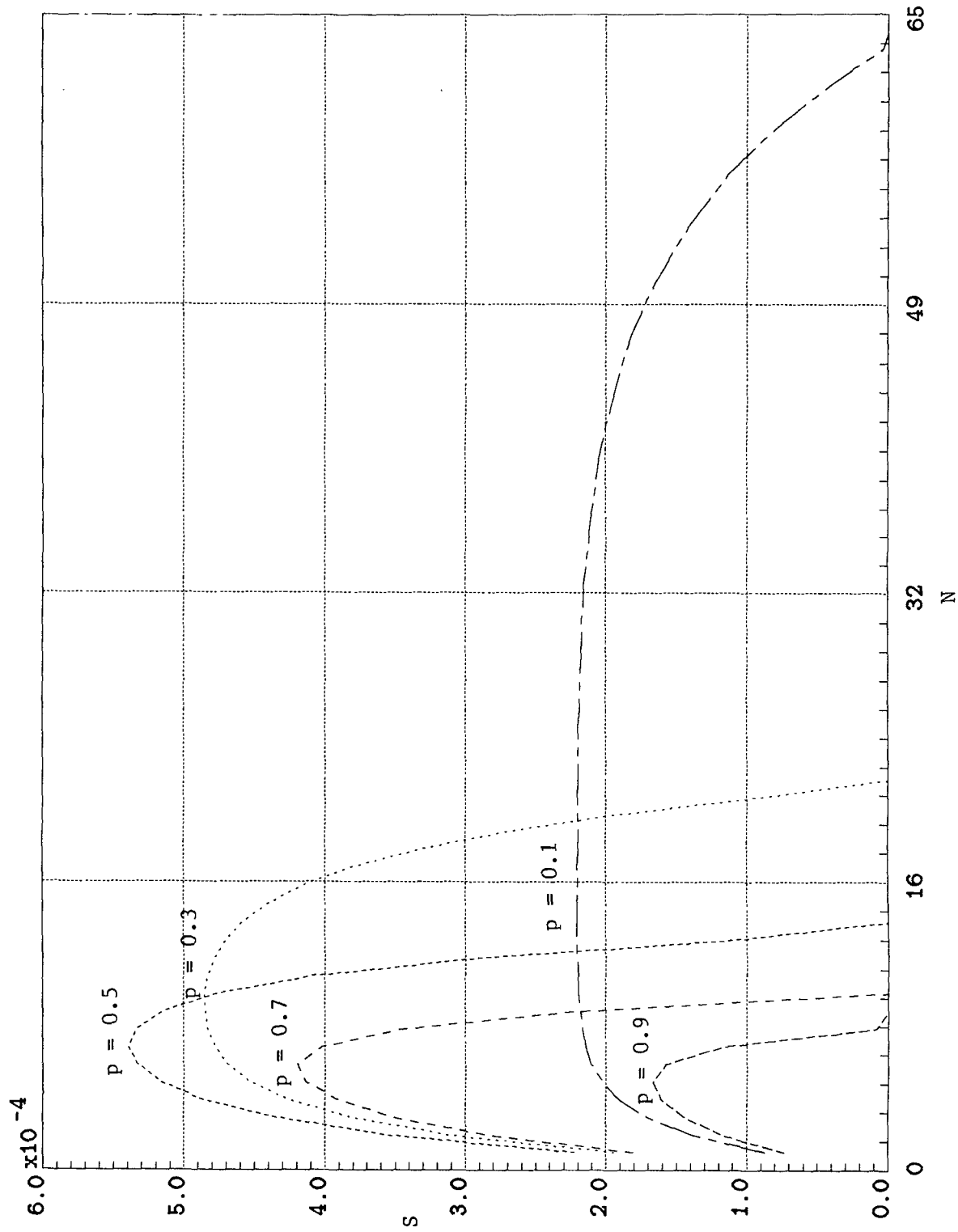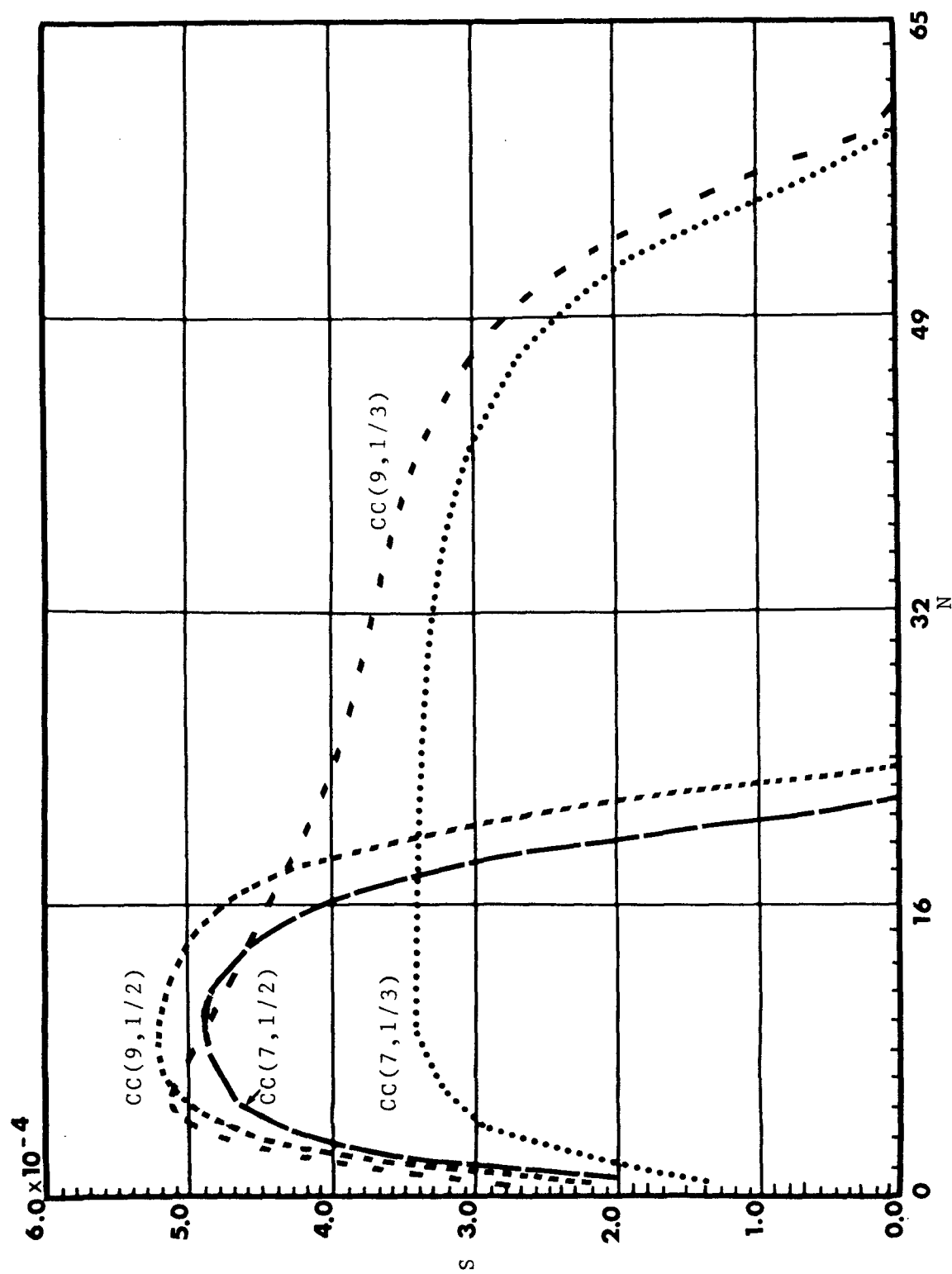
Figure 7(a). Throughput versus Average Number of Neighbors for Various p (RFR, $\lambda=0.1$, CC(7,1/2) coding with no side information available to the decoder, $q=100$, $N_b=10$, SNR=20 dB, AWGN, binary FSK with non-coherent demodulation, asynchronous).
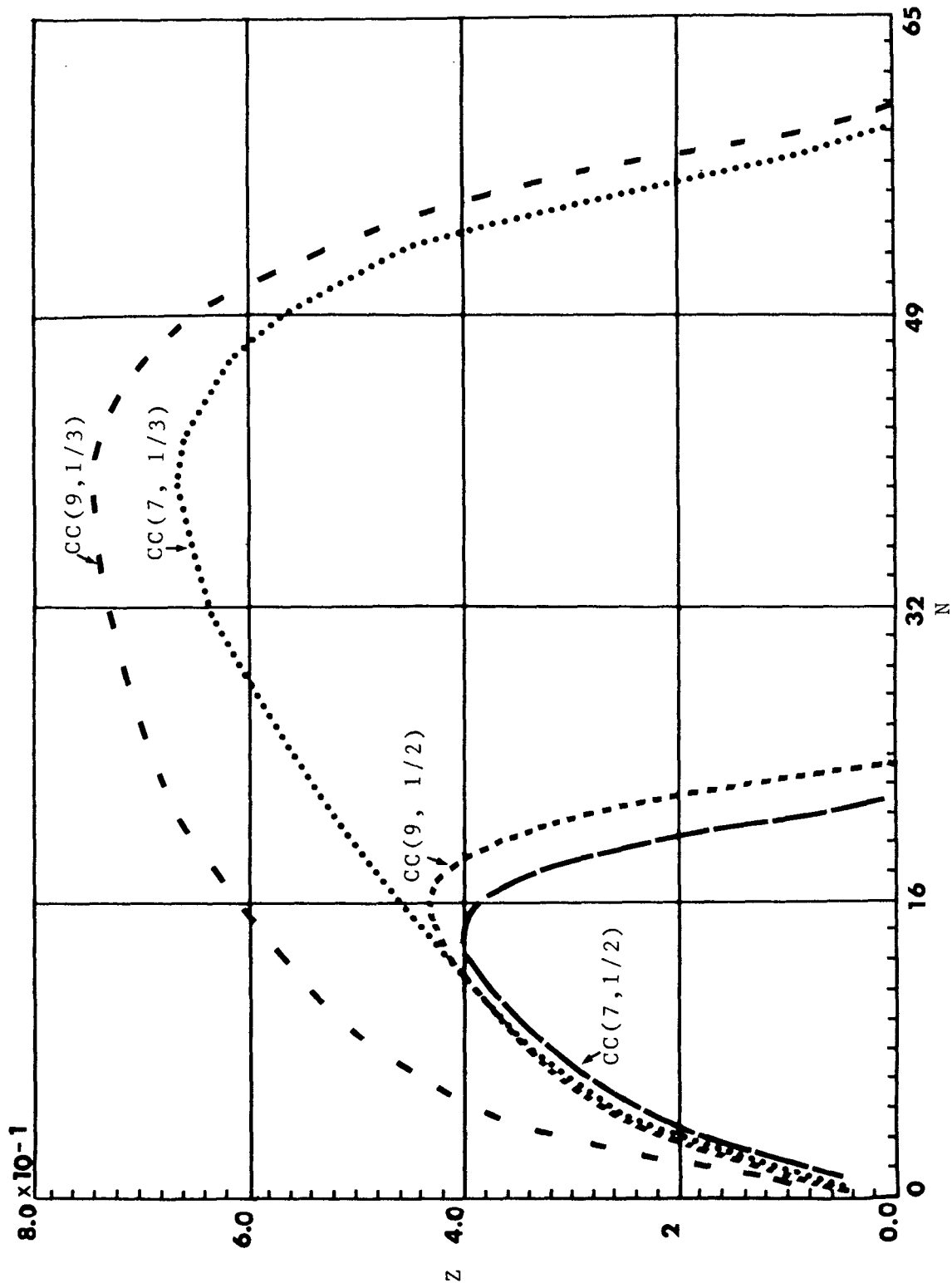
Figure 7(b). Expected Forward Progress versus Average Number of Neighbors for Various p (RFR, $\lambda=0.1$, CC(7,1/2) coding with no side information available to the decoder, q=100, $N_b=10$, SNR=20 dB, AWGN, binary FSK with non-coherent demodulation, asynchronous).

Figure 8(a).   Throughput versus Average Number of Neighbors for Various Binary Convolutional Codes (p=0.3, λ=0.1, no side information available to the decoder, q=100, N_b=10, SNR=20 dB, AWGN, binary FSK with non-coherent demodulation, asynchronous).
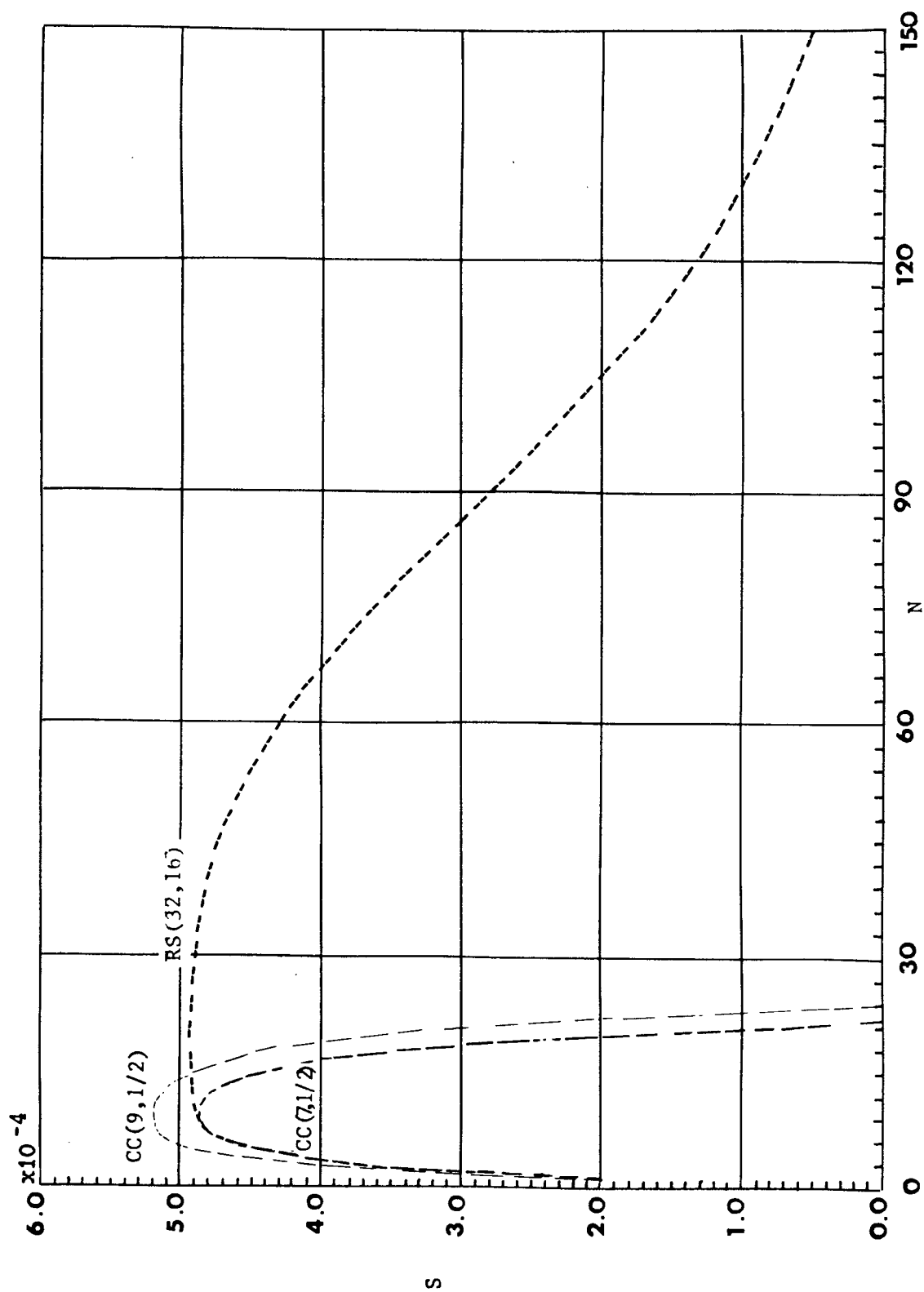
Figure 8(b). Expected Forward Progress versus Number of Neighbors for Various Binary Convolutional Codes ($p=0.3$, $\lambda=0.1$, no side information available to the decoder, $q=100$, $N_b=10$, SNR=20 dB, AWGN, binary FSK with non-coherent demodulation, asynchronous).

Figure 9(a). Throughput versus Average Number of Neighbors: Comparison of Binary Coding Schemes (RFR, p=0.3, λ=0.1, no side information available to the decoder (error-only correction in the Reed-Solomon case), q=100, N_b=10, SNR=20 dB, AWGN, binary FSK with non-coherent demodulation, asynchronous).
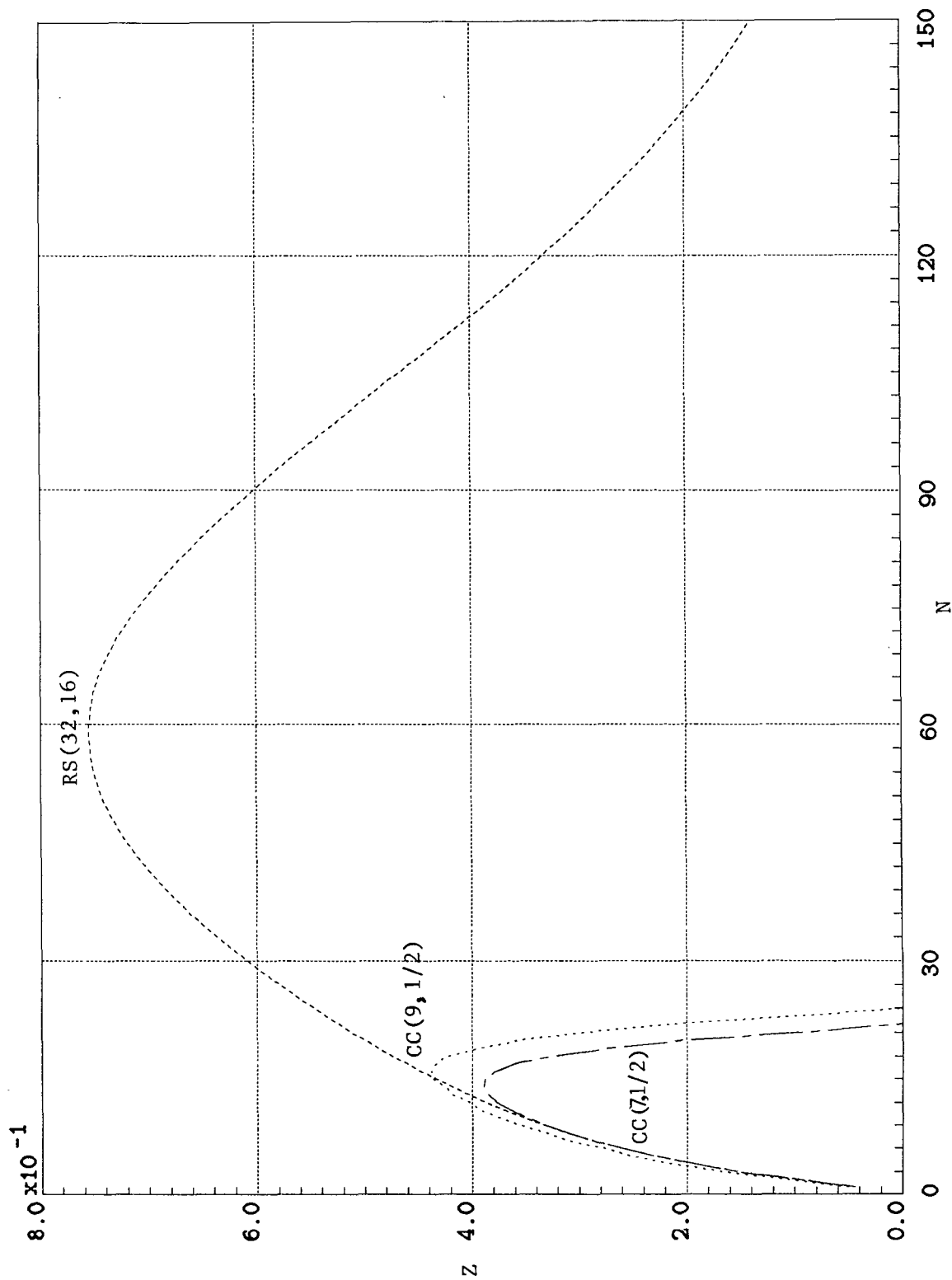
Figure 9(b).   Expected Forward Progress versus Average Number of Neighbors: Comparison of Binary Coding Schemes (RFR, p=0.3, λ=0.1, no side information available to the decoder (error—only correction in the Reed-Solomon case), q=100, N_b=10, SNR=20 dB, AWGN, binary FSK with non-coherent demodulation, asynchronous).
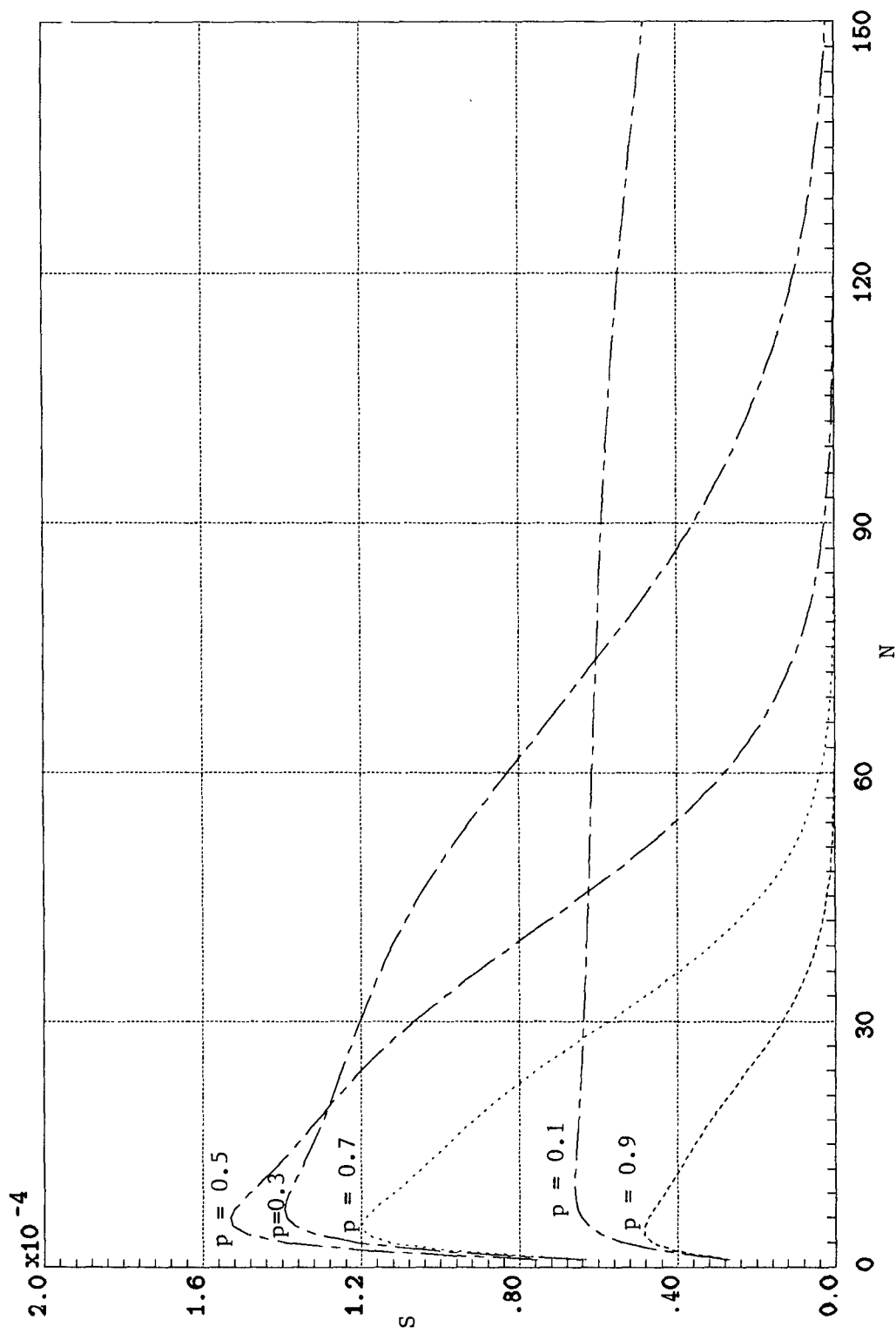
Figure 10(a). Throughput versus Average Number of Neighbors for Various p (MFR, $\lambda=0.1$, RS(32,16) coding with error-only decoding, $q=100$, $N_b=10$, SNR=20 dB, AWGN, 32-ary FSK with non-coherent demodulation, asynchronous).
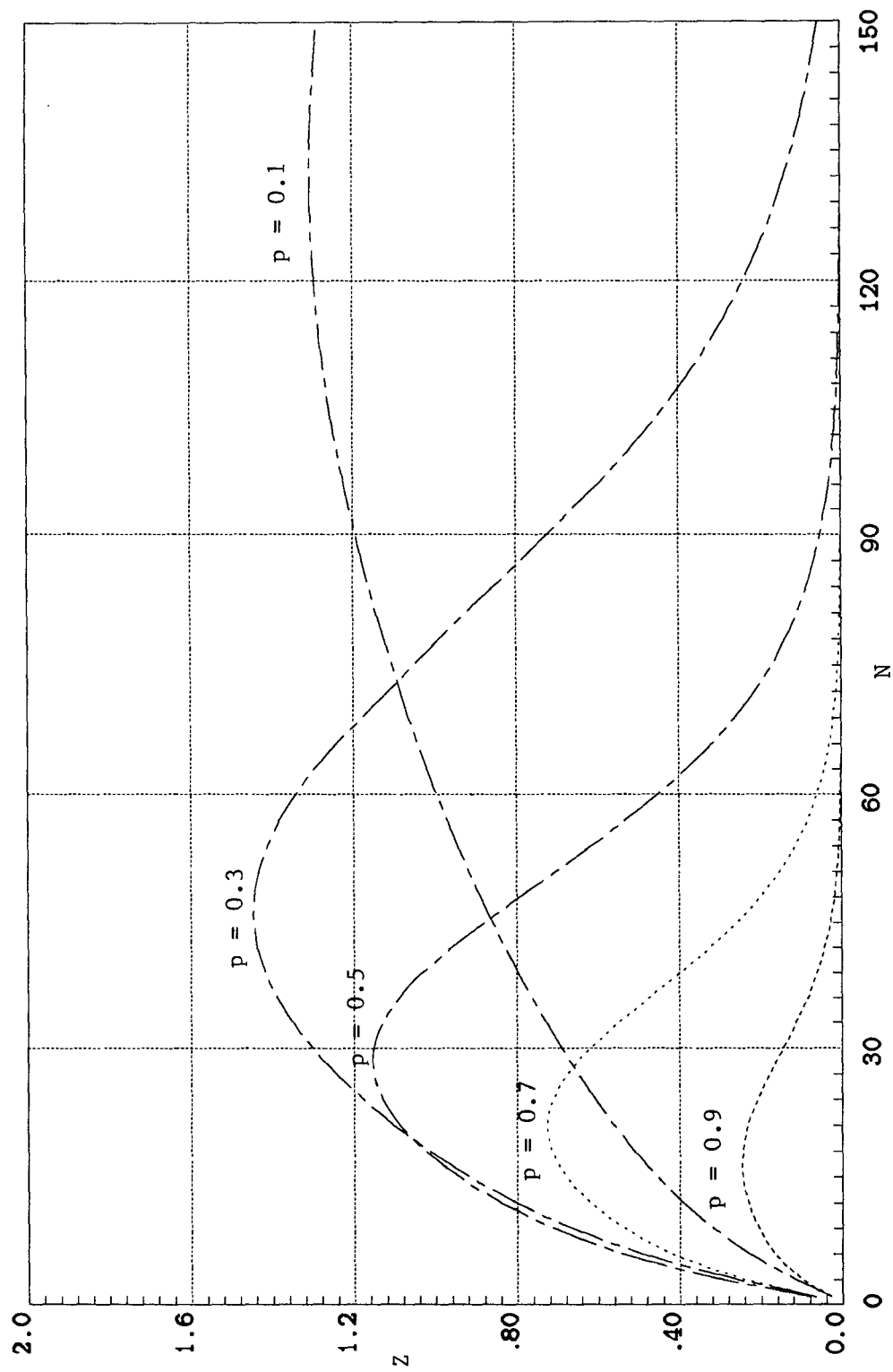
Figure 10(b). Expected Forward Progress versus Average Number of Neighbors for Various p (MFR, $\lambda=0.1$, RS(32,16) coding with error-only decoding, q=100, N_b=10, SNR=20 dB, AWGN, 32-ary FSK with non-coherent demodulation, asynchronous).
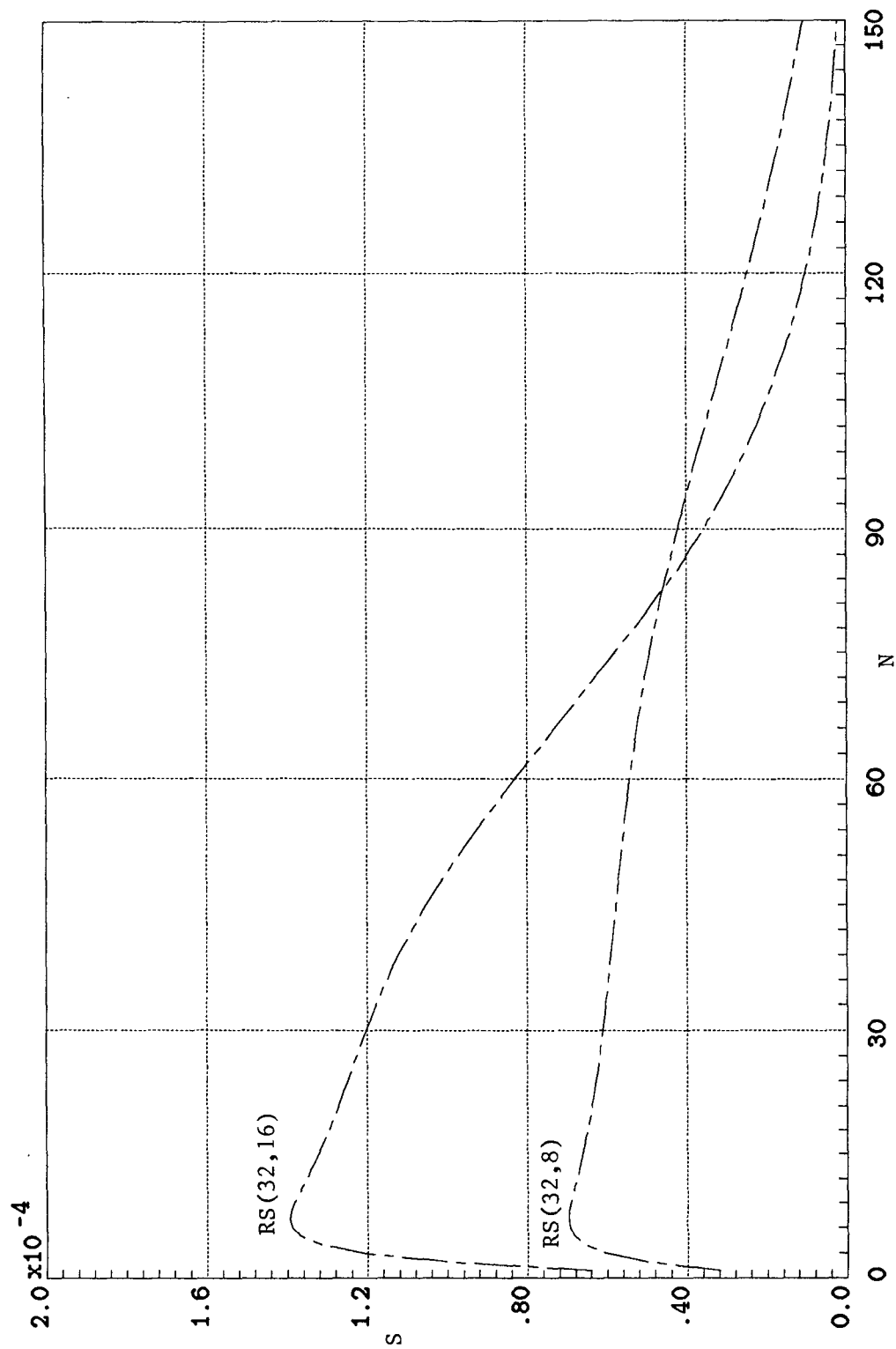
Figure 11(a). Throughput versus Average Number of Neighbors for Various Reed–Solomon Code Rates (MFR, p=0.3, λ=0.1, error –only decoding, q=100, N_b=10, SNR=20 dB, AWGN, 32–ary FSK with non–coherent demodulation, asynchronous).
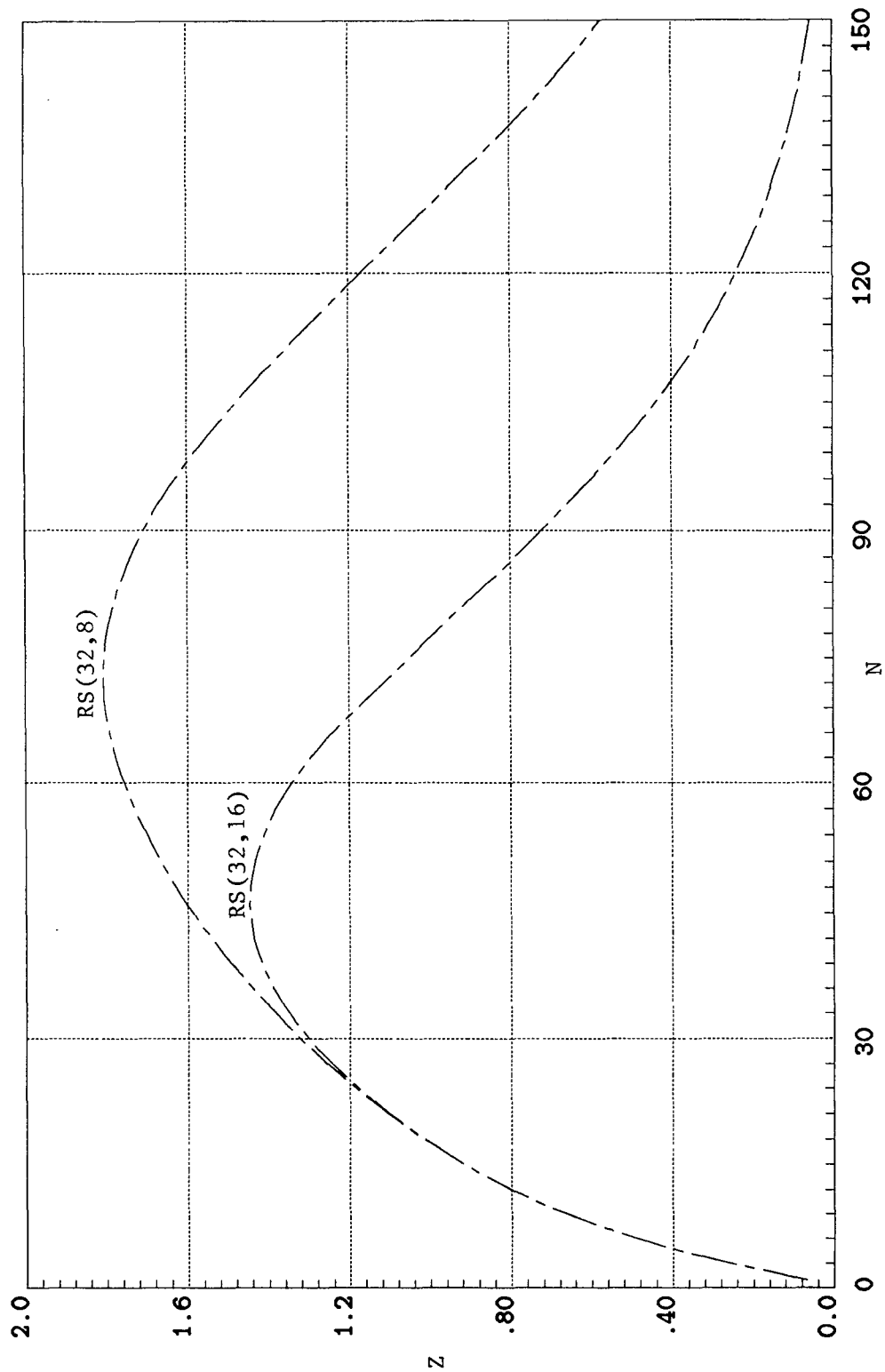
Figure 11(b). Expected Forward Progress versus Average Number of Neighbors for Various Reed-Solomon Code Rates (MFR, p=0.3, λ=0.1, error -only decoding, q=100, N_b=10, SNR=20 dB, AWGN, 32-ary FSK with non-coherent demodulation, asynchronous).
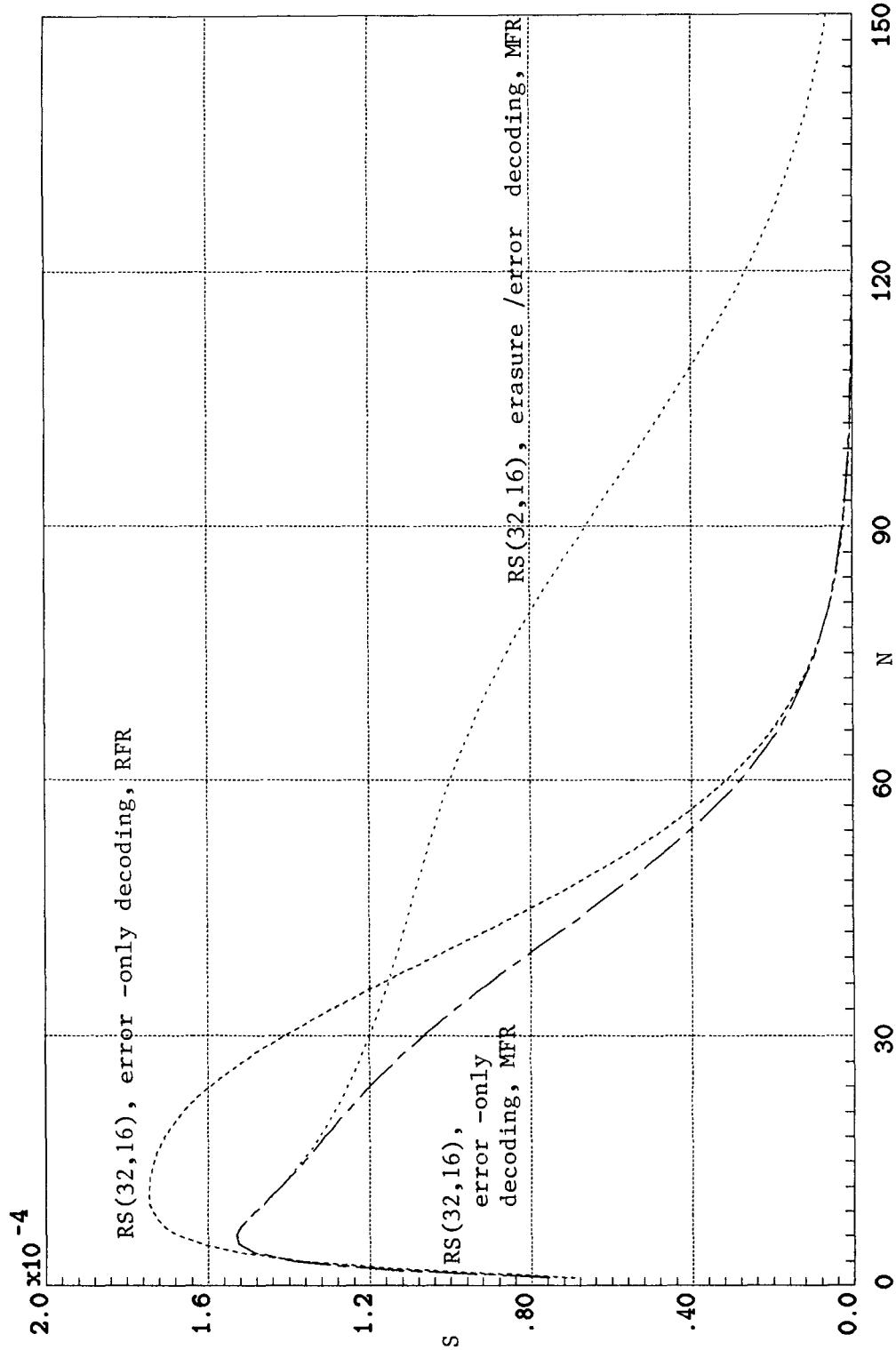
Figure 12(a).   Throughput versus Average Number of Neighbors for Comparable RFR and MFR Systems (p=0.5, λ=0.1, q=100, N_b=10, SNR=20 dB, AWGN, 32-ary FSK with non-coherent demodulation, asynchronous).
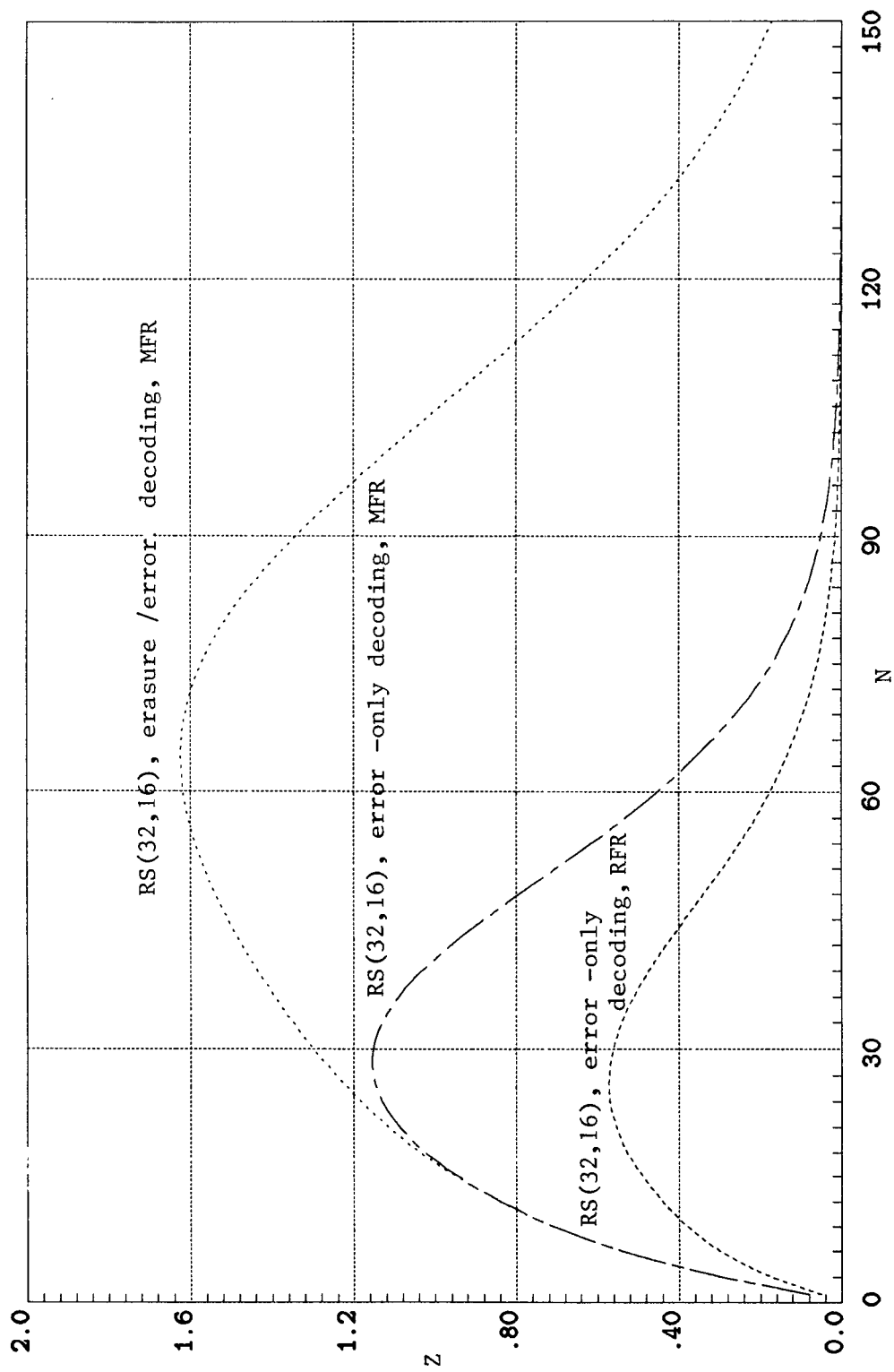
Figure 12(b). Expected Forward Progress versus Average Number of Neighbors for Comparable RFR and MFR Systems (p=0.5, λ=0.1, q=100, N_t=10, SNR=20 dB, AWGN, 32-ary FSK with non-coherent demodulation, asynchronous).

Appendix A: Derivation of Expressions for Coded RFR Systems

In Section II a result is stated for a Reed-Solomon coded RFR system. In this appendix, it will be shown exactly how this, as well as other results for coded RFR systems, can be determined.

In Section II a general result for RFR systems is derived. We have that

$$P(X \to Y) = P_{TX}(X \to Y)P_{I/TX}(X \to Y)$$

$$= p\left(1-e^{-\frac{N}{2}}\right)(1-p)\sum_{k=0}^{\infty}\frac{e^{-N}N^k}{k!}\sum_{j=0}^{k}\binom{k}{j}\left[1-p\left(1-e^{-\frac{N}{2}}\right)\right]^{k-j}$$

$$\sum_{i=0}^{j}\binom{j}{i}\left(\frac{p}{N}\right)^i\frac{1}{i+1}\left[p\left(1-e^{-\frac{N}{2}}\right)-\frac{p}{N}\right]^{j-i}P_c(j-i). \qquad (A.1)$$

In that same section, it is stated that $\dfrac{1}{i+1}$ can be closely approximated by a sum of exponentials of the form $\sum_{\nu}c_{\nu}\delta_{\nu}^{i}$, where $\delta_{\nu} = e^{\gamma_{\nu}}$ in the notation used in that section. A three term approximation is used here.

In order to obtain a closed-form expression, we must have $P_c(j-i)$ such that the dependency on $j-i$ is exponential; for example, if $P_c(j-i) = \sum_{m,l}b_{m,l}\,a_{m,l}^{j-i}$, this requirement would be satisfied. Having $P_c(j-i)$ in such a form, results in the final sum in (A.1) having the form of a binomial expansion. Several coding schemes, including those used here (Reed-Solomon and binary convolutional), result in a $P_c(j-i)$, of the required form.

We shall first consider **Reed-Solomon coding** $RS(n,k)$ **with error-correction decoding.** In this case, we have

$$P_c(j-i)= \sum_{m=0}^{t} \binom{n}{m} \left[p_s(j-i) \right]^m \left[1-p_s(j-i) \right]^{n-m}, \tag{A.2}$$

where $t = \left\lfloor \dfrac{n-k}{2} \right\rfloor$ is the error-correction capability of the $RS(n,k)$ code and $p_s(j-i)$ is

the probability of a symbol error. Furthermore, $p_s(j-i)$ can be bounded/ approximated

by

$$p_s(j-i) \le 1-(1-P_0)(1-P_h)^{j-i} \tag{A.3}$$

for codes over $GF(M^1)$ [$(1-P_0)$ becomes $(1-P_0)^{m_c}$ for codes over $GF(M^{m_c})$], where P_0 is

the probability of symbol error (without multi-user interference) and P_h is the probabil-

ity of a symbol being hit (interferred with by another user's transmission, given by [8]

$$P_h = \frac{1}{q} \left(1 + \frac{m_c \log_2 M}{N_b} \right)$$

for random hopping pattern assignments. Here, q is the number of available hopping

frequencies, N_b is the number of bits per hop, and M^{m_c} is the order of the field over

which the code is defined.

Using (A.3), (A.2) can be written as

$$P_c(j-i) = \sum_{m=0}^{t} \binom{n}{m} \left[1-(1-P_0)(1-P_h)^{j-i} \right]^m \left[(1-P_0)(1-P_h)^{j-i} \right]^{n-m}$$

$$= \sum_{m=0}^{t} \sum_{l=0}^{m} \binom{n}{m}\binom{m}{l}(-1)^l \left[(1-P_0)(1-P_h)^{j-i} \right]^l \left[(1-P_0)(1-P_h)^{j-i} \right]^{n-m}$$

$$= \sum_{m=0}^{t} \sum_{l=0}^{m} \binom{n}{m}\binom{m}{l}(-1)^l (1-P_0)^{n+l-m} \left[(1-P_h)^{n+l-m} \right]^{j-i}. \tag{A.4}$$

(A.4) has the form discussed above. We now use (A.4) and the aforementioned exponen-

tial approximation to $\dfrac{1}{i+1}$ in (A.1) to yield

$$P(X \rightarrow Y) = p\left(1-e^{-\frac{N}{2}}\right)(1-p)\sum_{\nu=1}^{3} c_{\nu} \sum_{m=0}^{t} \sum_{l=0}^{m} \binom{n}{m}\binom{m}{l}(-1)^{l}(1-P_{0})^{n+l+m}\sum_{k=0}^{\infty}\frac{e^{-N}N^{k}}{k!}$$

$$\sum_{j=0}^{k}\binom{k}{j}\left[1-p\left(1-e^{-\frac{N}{2}}\right)\right]^{k-j}p^{j}\sum_{i=0}^{j}\binom{j}{i}\left(\frac{\delta_{\nu}}{N}\right)^{i}\left[\left(1-e^{-\frac{N}{2}}-\frac{1}{N}\right)(1-P_{h})^{n+l-m}\right]^{j-i}$$

$$= p\left(1-e^{-\frac{N}{2}}\right)(1-p)\sum_{\nu=1}^{3} c_{\nu} \sum_{m=0}^{t} \sum_{l=0}^{m} \binom{n}{m}\binom{m}{l}(-1)^{l}(1-P_{0})^{n+l-m}\sum_{k=0}^{\infty}\frac{e^{-N}N^{k}}{k!}$$

$$\sum_{j=0}^{k}\binom{k}{j}\left[1-p\left(1-e^{-\frac{N}{2}}\right)\right]^{k-j}\left\{p\left[\frac{\delta_{\nu}}{N}+\left(1-e^{-\frac{N}{2}}-\frac{1}{N}\right)(1-P_{h})^{n+l-m}\right]\right\}^{j}$$

$$= p\left(1-e^{-\frac{N}{2}}\right)(1-p)\sum_{\nu=1}^{3} c_{\nu} \sum_{m=0}^{t} \sum_{l=0}^{m} \binom{n}{m}\binom{m}{l}(-1)^{l}(1-P_{0})^{n+l-m} e^{-N}$$

$$\sum_{k=0}^{\infty}\frac{1}{k!}\left\{N\left[1-p\left(1-e^{-\frac{N}{2}}-\frac{\delta_{\nu}}{N}-\left(1-e^{-\frac{N}{2}}-\frac{1}{N}\right)(1-P_{h})^{n+l-m}\right)\right]\right\}^{k}$$

$$= p\left(1-e^{-\frac{N}{2}}\right)(1-p)\sum_{\nu=1}^{3} c_{\nu} \sum_{m=0}^{t} \sum_{l=0}^{m} \binom{n}{m}\binom{m}{l}(-1)^{l}(1-P_{0})^{n+l-m}$$

$$\exp\left\{-pN\left[1-e^{-\frac{N}{2}}-\frac{\delta_{\nu}}{N}-\left(1-e^{-\frac{N}{2}}-\frac{1}{N}\right)(1-P_{h})^{n+l-m}\right]\right\}. \qquad (A.5)$$

This exactly the expression given as eq. (6) in Section II.

The expression for $RS(n,k)$ **Reed-Solomon coding with erasure/error-correction decoding** can be obtained in a similar fashion. In this case, $P_{c}(j-i)$ is given by (see, for example, [9])

$$P_{c}(j-i)=1- \sum_{\substack{\eta+\varsigma\leq n \\ e+1\leq 2\varsigma+\eta}} \binom{n}{\varsigma}\binom{n-\varsigma}{\eta}\left[p_{s}(j-i)\right]^{\varsigma}\left[\epsilon_{s}(j-i)\right]^{\eta}\left[1-p_{s}(j-i)-\epsilon_{s}(j-i)\right]^{n-\eta-\varsigma}, (A.6)$$

where $e=n-k$, $\epsilon_{s}(j-i)$ is the symbol erasure probability given by

$$\epsilon_{s}(j-i)=1-(1-P_{h})^{j-i},$$

and $p_{s}(j-i)$, the symbol error probability, is given by

$$p_s(j-i) = P_0(1-P_h)^{j-i}$$

for codes over $GF(M^1)$ [the P_0 would become $1-(1-P_0)^{m_c}$ for codes over $GF(M^{m_c})$].

Substituting into (A.1) and proceeding as above, we obtain

$$P(X \to Y) = p\left(1-e^{-\frac{N}{2}}\right)(1-p)\sum_{v=1}^{3}c_v\left[\exp[p(\delta_v-1)]-\sum_{\mu=0}^{n}\sum_{\substack{m=max\left\{0,e+1-2\mu\right\}}}^{n-\mu}\sum_{l=0}^{\eta}\binom{n}{\mu}\binom{n-\mu}{\eta}\binom{\eta}{l}\right.$$

$$\left.(-1)^l P_0^{\mu}(1-P_0)^{n-\mu-\eta}\exp\left\{-pN\left[1-e^{-\frac{N}{2}}\frac{\delta_v}{N}-\left(1-e^{-\frac{N}{2}}-\frac{1}{N}\right)(1-P_h)^{n+l-\eta}\right]\right\}\right].$$

$$(A.7)$$

For **binary convolutional codes** with Viterbi decoding and hard decisions, $P_c(j-i)$ can be bounded/approximated by (see, for example, [10])

$$P_c(j-i) \leq 1 - r_c \sum_{\mu=d_{free}}^{\infty} w_{\mu}P_{\mu}$$

where

$$P_{\mu} = \begin{cases} P_2(\mu;p(j-i)), & \text{no side information} \\ \left[\epsilon_s(j-i)\right]^{\mu}P_2(\mu;\overline{p})+\sum_{l=0}^{\mu-1}\binom{\mu}{l}\left[\epsilon_s(j-i)\right]^{\mu-l}P_2(\mu-l;P_0), & \text{with side information,} \end{cases}$$

$$(A.8)$$

where r_c is the code rate, d_{free} is the free distance of the code, w_{μ} is the total information weight of all sequences which produce paths of weight μ, P_0 is as described above, $p(j-i)=1-(1-P_0)(1-P_h)^{j-i}$, $\overline{p}=\frac{1}{2}$, and $\epsilon_s(j-i)=1-(1-P_h)^{j-i}$. $P_2(n;q)$ is defined as

$$P_2(n;q) = \begin{cases} \displaystyle\sum_{l=\frac{n+1}{2}}^{n} \binom{n}{l} q^l(1-q)^{n-l}, & n \text{ odd} \\[2em] \displaystyle\sum_{l=\frac{n}{2}+1}^{n} \binom{n}{l} q^l(1-q)^{n-l} + \frac{1}{2}\binom{n}{\frac{n}{2}} \left[q(1-q)\right]^{\frac{n}{2}}, & n \text{ even.} \end{cases}$$

It should be noted that the summation over μ in (A.8) generally involves only a few non-zero terms.

Substituting (A.8) into (A.1) and proceeding as above, the following result is obtained:

$$P(X \to Y) = p\left(1-e^{-\frac{N}{2}}\right)(1-p)\sum_{\nu=1}^{3} c_\nu \left[\exp[-p(1-\delta_\nu)] - r_c \sum_{\mu=d_{free}}^{\infty} w_\mu Q_\mu\right], \qquad (A.9)$$

where for the case in which **no side information is available**,

$$Q_\mu = \sum_{\rho=\frac{\mu+1}{2}}^{\mu} \sum_{\eta=0}^{\rho} \binom{\mu}{\rho}\binom{\rho}{\eta}(-1)^\eta(1-P_0)^{\mu+\eta-\rho}\exp\left\{-pN\left[1-e^{-\frac{N}{2}}-\frac{\delta_\nu}{N}\left(1-e^{-\frac{N}{2}}-\frac{1}{N}\right)(1-P_h)^{\mu+\eta-\rho}\right]\right\},$$

$$(A.10a)$$

if μ is odd, and

$$Q_\mu = \sum_{\rho=\frac{\mu}{2}+1}^{\mu} \sum_{\eta=0}^{\rho} \binom{\mu}{\rho}\binom{\rho}{\eta}(-1)^\eta(1-P_0)^{\mu+\eta-\rho}\exp\left\{-pN\left[1-e^{-\frac{N}{2}}-\frac{\delta_\nu}{N}\left(1-e^{-\frac{N}{2}}-\frac{1}{N}\right)(1-P_h)^{\mu+\eta-\rho}\right]\right\}$$

$$+ \frac{1}{2}\binom{\mu}{\frac{\mu}{2}}\sum_{\rho=0}^{\frac{\mu}{2}}\binom{\frac{\mu}{2}}{\rho}(-1)^\rho(1-P_0)^{\rho+\frac{\mu}{2}}\exp\left\{-pN\left[1-e^{-\frac{N}{2}}-\frac{\delta_\nu}{N}\left(1-e^{-\frac{N}{2}}-\frac{1}{N}\right)(1-P_h)^{\rho+\frac{\mu}{2}}\right]\right\},$$

$$(A.10b)$$

if μ is even; whereas for the case in which **side information is available**,

$$Q_\mu = P_2(\mu;\frac{1}{2})\sum_{\eta=0}^{\mu}\binom{\mu}{\eta}(-1)^\eta\exp\left\{-pN\left[1-e^{-\frac{N}{2}}-\frac{\delta_\nu}{N}\left(1-e^{-\frac{N}{2}}-\frac{1}{N}\right)(1-P_h)^\eta\right]\right\}$$

$$+ \sum_{\lambda=0}^{\mu} \binom{\mu}{\lambda} P_2(\mu-\lambda;P_0) \sum_{\sigma=0}^{\lambda} \binom{\lambda}{\sigma} (-1)^\sigma \exp\left\{ -pN\left[1-e^{-\frac{N}{2}} \frac{\delta_\nu}{N} \left(1-e^{-\frac{N}{2}} - \frac{1}{N} \right) (1-P_h)^{\mu+\sigma-\lambda} \right] \right\}.$$

$$(A.11)$$

Note that $P_2(\mu;\frac{1}{2})$ and $P_2(\mu-\lambda;P_0)$ have not been expanded, since each is a constant for

a given value of μ or $(\mu-\lambda)$, respectively.

Appendix B : Derivation of Expressions for Coded MFR Systems

As in Appendix A, above, we will show, in detail, how closed-form results have been obtained for the same codes treated in Appendix A, but in an MFR system. The expressions for $P_c(j-i)$ are exactly as stated in Appendix A and will not be repeated here. The result for binary convolutional coding with side information available at the decoder will be derived in detail, and the other results will be stated, for the sake of completeness.

In Section III the following formula is derived:

$$P(X \to Y) = p\left(1-e^{-\frac{N}{2}}\right)(1-p)$$

$$\int_0^R \int_{-\frac{\pi}{2}}^{\frac{\pi}{2}} \sum_{k=0}^{\infty} e^{-N'(r_0,\theta_0)} \frac{[N'(r_0,\theta_0)]^k}{k!} \sum_{j=0}^{k} \binom{k}{j} \left[p\left(1-e^{-\frac{N}{2}}\right)\right]^j \left[1-p\left(1-e^{-\frac{N}{2}}\right)\right]^{k-j}$$

$$\sum_{i=0}^{j} \binom{j}{i} \frac{1}{i+1} \left[P_1(R)\right]^i \left[1-P_1(R)\right]^{j-i} P_c(j-i)$$

$$f_{r,\theta}(r_0,\theta_0)d\theta_0 dr_0. \tag{B.1}$$

As in Appendix A, we will use the three term exponential approximation to $\frac{1}{i+1}$, $\sum_{\nu=1}^{3} c_\nu \delta_\nu^i$. For convenience, let use define $I_\nu(r_0,\theta_0)$ by

$$I_\nu(r_0,\theta_0) = \sum_{k=0}^{\infty} e^{-N'(r_0,\theta_0)} \frac{[N'(r_0,\theta_0)]^k}{k!} \sum_{j=0}^{k} \binom{k}{j} \left[p\left(1-e^{-\frac{N}{2}}\right)\right]^j \left[1-p\left(1-e^{-\frac{N}{2}}\right)\right]^{k-j}$$

$$\sum_{i=0}^{j} \binom{j}{i} \left[\delta_\nu P_1(R)\right]^i \left[1-P_1(R)\right]^{j-i} P_c(j-i); \tag{B.2}$$

It is clear that this includes all that varies from one code to another, and therefore, all of the results with be stated in terms of $I_\nu(r_0,\theta_0)$. Note that, by definition,

$$P(X \rightarrow Y) = p\left(1-e^{-\frac{N}{2}}\right)(1-p)\sum_{\nu=1}^{3} c_\nu \int_0^R \int_{-\frac{\pi}{2}}^{\frac{\pi}{2}} I_\nu(r_0,\theta_0)f_{r,\theta}(r_0,\theta_0)d\theta_0 dr_0,$$

and, since expected forward process is computed by including $r_0\cos\theta_0$ in the integrand,

$$Z = p\left(1-e^{-\frac{N}{2}}\right)(1-p)\sum_{\nu=1}^{3} c_\nu \int_0^R \int_{-\frac{\pi}{2}}^{\frac{\pi}{2}} r_0\cos\theta_0 \, I_\nu(r_0,\theta_0) \, f_{r,\theta}(r_0,\theta_0)d\theta_0 dr_0.$$

Let us begin with the case of **binary convolutional coding with side informa-tion** available at the decoder. The expression for $P_c(j-i)$ is given in eq. (A.8). Before beginning the actual analysis, let us first observe that since $\bar{p}=\frac{1}{2}$ and P_0 is a constant, the factors involving $P_2(\cdot;\cdot)$ are independent of $(j-i)$; thus, it will not be necessary to expand them (as opposed to the case in which no side information is available to the decoder; the expression is of the form $P_2(\cdot;p(j-i))$ and must be expanded).

To start, let us manipulate $P_c(j-i)$ into a desirable form.

$$P_c(j-i) = 1 - r_c \sum_{\mu=d_{free}}^{\infty} w_\mu \left\{ \left[\epsilon_s(j-i)\right]^\mu P_2\left(\mu;\frac{1}{2}\right) + \sum_{\lambda=0}^{\mu=1}\binom{\mu}{\lambda}\left[\epsilon_s(j-i)\right]^{\mu-\lambda}P_2\left(\mu-\lambda;P_0\right) \right\}$$

$$= 1 - r_c \sum_{\mu=d_{free}}^{\infty} w_\mu \left\{ \left[1-(1-P_h)^{j-i}\right]^\mu P_2\left(\mu;\frac{1}{2}\right) \right.$$

$$\left. + \sum_{\lambda=0}^{\mu-1}\binom{\mu}{\lambda}\left[1-(1-P_h)^{j-i}\right]^\lambda\left[(1-P_h)^{j-i}\right]^{\mu-\lambda}P_2\left(\mu-\lambda;P_0\right) \right\}$$

$$= 1 - r_c \sum_{\mu=d_{free}}^{\infty} w_\mu \left\{ P_2\left(\mu;\frac{1}{2}\right)\sum_{\eta=0}^{\mu}\binom{\mu}{\eta}(-1)^\eta\left[(1-P_h)^\eta\right]^{j-i} \right.$$

$$+ \sum_{\lambda=0}^{\mu-1} \sum_{\sigma=0}^{\lambda} \binom{\mu}{\lambda}\binom{\lambda}{\sigma}(-1)^{\sigma}P_2\Big(\mu-\lambda;P_0\Big)\left[(1-P_h)^{\mu-\lambda+\sigma}\right]^{j-i}\Bigg\}.$$

(B.3)

We now have $P_c(j-i)$ depending on $(j-i)$ exponentially, as desired.

We can now substitute (B.3) into (B.2) and derive $I_\nu(r_0,\theta_0)$; however, the expression would be rather long. Instead, we will treat the three terms of (B.3) individually (we consider the leading 1 as a term). Looking at the first term, we have

$$I_\nu^{(1)}(r_0,\theta_0) = \sum_{k=0}^{\infty} e^{-N'(r_0,\theta_0)} \frac{[N'(r_0,\theta_0)]^k}{k!} \sum_{j=0}^{k}\binom{k}{j}\left[p\left(1-e^{-\frac{N}{2}}\right)\right]^j \left[1-p\left(1-e^{-\frac{N}{2}}\right)\right]^{k-j}$$

$$\sum_{i=0}^{j}\binom{j}{i}\left[\delta_\nu P_1(R)\right]^i \left[1-P_1(R)\right]^{j-i}$$

$$= \sum_{k=0}^{\infty} e^{-N'(r_0,\theta_0)} \frac{[N'(r_0,\theta_0)]^k}{k!} \sum_{j=0}^{k}\binom{k}{j}\left[p(1-e^{-\frac{N}{2}})\left[1-(1-\delta_\nu)P_1(R)\right]\right]^j \left[1-p(1-e^{-\frac{N}{2}})\right]^{k-j}$$

$$= \sum_{k=0}^{\infty} e^{-N'(r_0,\theta_0)} \frac{[N'(r_0,\theta_0)]^k}{k!} \left[1-p\left(1-e^{-\frac{N}{2}}\right)(1-\delta_\nu)P_1(R)\right]^k$$

$$= \exp\left\{-pN'(r_0,\theta_0)\left(1-e^{-\frac{N}{2}}\right)(1-\delta_\nu)P_1(R)\right\}.$$

(B.4)

From the second term, we get

$$I_\nu^{(2)}(r_0,\theta_0) = r_c \sum_{\mu=d_{free}}^{\infty} w_\mu P_2\left(\mu;\frac{1}{2}\right)\sum_{\eta=0}^{\mu}\binom{\mu}{\eta}(-1)^\eta \sum_{k=0}^{\infty} e^{-N'(r_0,\theta_0)}\frac{[N'(r_0,\theta_0)]^k}{k!}\sum_{j=0}^{k}\binom{k}{j}\left[p\left(1-e^{-\frac{N}{2}}\right)\right]^j$$

$$\left[1-p\left(1-e^{-\frac{N}{2}}\right)\right]^{k-j}\sum_{i=0}^{j}\binom{j}{i}\left[\delta_\nu P_1(R)\right]^i\left[(1-P_1(R))(1-P_h)^\eta\right]^{j-i}$$

$$= r_c \sum_{\mu=d_{free}}^{\infty} w_\mu P_2\left(\mu;\frac{1}{2}\right)\sum_{\eta=0}^{\mu}\binom{\mu}{\eta}(-1)^\eta \sum_{k=0}^{\infty} e^{-N'(r_0,\theta_0)}\frac{[N'(r_0,\theta_0)]^k}{k!}$$

$$\sum_{j=0}^{k} \binom{k}{j} \left[p\left(1-e^{-\frac{N}{2}}\right)\left(\delta_\nu P_1(R)+[1-P_1(R)](1-P_h)^\eta\right) \right]^j \left[1-p\left(1-e^{-\frac{N}{2}}\right) \right]^{k-j}$$

$$= r_c \sum_{\mu=d_{free}}^{\infty} w_\mu P_2\left(\mu;\frac{1}{2}\right) \sum_{\eta=0}^{\mu} \binom{\mu}{\eta}(-1)^\eta \sum_{k=0}^{\infty} e^{-N'(r_0,\theta_0)} \frac{[N'(r_0,\theta_0)]^k}{k!}$$

$$\left\{ 1-p\left(1-e^{-\frac{N}{2}}\right)\left[1-\delta_\nu P_1(R)-[1-P_1(R)](1-P_h)^\eta\right] \right\}^k$$

$$= r_c \sum_{\mu=d_{free}}^{\infty} w_\mu P_2\left(\mu;\frac{1}{2}\right) \sum_{\eta=0}^{\mu} \binom{\mu}{\eta}(-1)^\eta$$

$$\exp\left\{ -pN'(r_0,\theta_0)\left(1-e^{-\frac{N}{2}}\right)\left[1-\delta_\nu P_1(R)-[1-P_1(R)](1-P_h)^\eta\right] \right\}.$$

(B.5)

Since the analysis of the third term is nearly exactly the same as that of the second term, the result will simply be stated:

$$I_\nu^{(3)}(r_0,\theta_0) = r_c \sum_{\mu=d_{free}}^{\infty} w_\mu \sum_{\lambda=0}^{\mu-1}\sum_{\sigma=0}^{\lambda} \binom{\mu}{\lambda}\binom{\lambda}{\sigma}(-1)^\sigma P_2\left(\mu-\lambda;P_0\right)$$

$$\exp\left\{ -pN'(r_0,\theta_0)\left(1-e^{-\frac{N}{2}}\right)\left[1-\delta_\nu P_1(R)-[1-P_1(R)](1-P_h)^{\mu-\lambda+\sigma}\right] \right\}.$$

(B.6)

$I_\nu(r_0,\theta_0)$ is obtained by taking $I_\nu(r_0,\theta_0) = I_\nu^{(1)}(r_0,\theta_0) - I_\nu^{(2)}(r_0,\theta_0) - I_\nu^{(3)}(r_0,\theta_0)$.

For the other three coding schemes considered here, the results are as follows:

1. For $RS(n,k)$ **Reed-Solomon coding with error-correction decoding,**

$$I_\nu(r_0,\theta_0) = \sum_{m=0}^{t} \sum_{l=0}^{m} \binom{n}{m}\binom{m}{l}(-1)^l (1-P_0)^{n+l-m}$$

$$\exp\left\{-pN'(r_0,\theta_0)\left(1-e^{-\frac{N}{2}}\right)\left[1-\delta_\nu P_1(R)-[1-P_1(R)](1-P_h)^{n+l-m}\right]\right\}.$$

(B.7)

2. For $RS(n,k)$ **Reed-Solomon coding with erasure/error-correction decoding**, use $I_\nu^{(1)}(r_0,\theta_0)$ in (B.4) and $I_\nu(r_0,\theta_0) = I_\nu^{(1)}(r_0,\theta_0) - I_\nu^{(2)}(r_0,\theta_0)$, where

$$I_\nu^{(2)}(r_0,\theta_0) = \sum_{\mu=0}^{n} \sum_{\eta=\max\left\{0,e+1-2\mu\right\}}^{n-\mu} \sum_{l=0}^{\eta} \binom{n}{\mu}\binom{n-\mu}{\eta}\binom{\eta}{l}(-1)^{n-\mu-\eta}$$

$$\exp\left\{-pN'(r_0,\theta_0)\left(1-e^{-\frac{N}{2}}\right)\left[1-\delta_\nu P_1(R)-[1-P_1(R)](1-P_h)^{n+l-\eta}\right]\right\}.$$

(B.8)

Note that for both $RS(n,k)$ coding cases, the results are shown for codes over $GF(M^1)$.

For codes over $GF(M^{m_c})$, replace $(1-P_0)$ in both cases by $(1-P_0)^{m_c}$, and, in (B.8), replace the factor of P_0^μ by a factor of $[1-(1-P_0)^{m_c}]^\mu$.

3. For **binary convolutional coding with no side information** available to the decoder, we have $I_\nu^{(1)}(r_0,\theta_0)$ as in (B.4),

$$I_\nu^{(2)}(r_0,\theta_0) = r_c \sum_{\mu=d_{free}}^{\infty} w_\mu P_\mu$$

(B.9)

where, if μ is odd,

$$P_\mu = \sum_{\rho=\frac{\mu+1}{2}}^{\mu} \sum_{\eta=0}^{\rho} \binom{\mu}{\rho}\binom{\rho}{\eta}(-1)^\eta (1-P_0)^{\mu+\eta-\rho}$$

$$\exp\left\{-pN'\ (r_0,\theta_0)\left(1-e^{-\frac{N}{2}}\right)\left[1-\delta_\nu P_1(R\ )-[1-P_1(R\ )](1-P_h\ )^{\mu+\eta-\rho}\right]\right\},$$

<div align="right">(B.10a)</div>

and, if μ is eveni,

$$P_\mu = \sum_{\rho=\frac{\mu}{2}+1}^{\mu}\sum_{\eta=0}^{\rho}\binom{\mu}{\rho}\binom{\rho}{\eta}(-1)^\eta(1-P_0)^{\mu+\eta-\rho}$$

$$\exp\left\{-pN'\ (r_0,\theta_0)\left(1-e^{-\frac{N}{2}}\right)\left[1-\delta_\nu P_1(R\ )-[1-P_1(R\ )](1-P_h\ )^{\mu+\eta-\rho}\right]\right\}$$

$$+\frac{1}{2}\binom{\mu}{\frac{\mu}{2}}\sum_{\rho=0}^{\frac{\mu}{2}}\binom{\frac{\mu}{2}}{\rho}(-1)^\rho(1-P_0)^{\rho+\frac{\mu}{2}}$$

$$\exp\left\{-pN'\ (r_0,\theta_0)\left(1-e^{-\frac{N}{2}}\right)\left[1-\delta_\nu P_1(R\ )-[1-P_1(R\ )](1-P_h\ )^{\rho+\frac{\mu}{2}}\right]\right\},$$

<div align="right">(B.10b)</div>

and, as before, $I_\nu(r_0,\theta_0) = I_\nu^{(1)}\ (r_0,\theta_0) - I_\nu^{(2)}\ (r_0,\theta_0)$.